Master thesis

Design and testing of a single catalyst particle diagnostic platform at elevated temperature and pressure

By Jeroen Vollenbroek (s1096214)

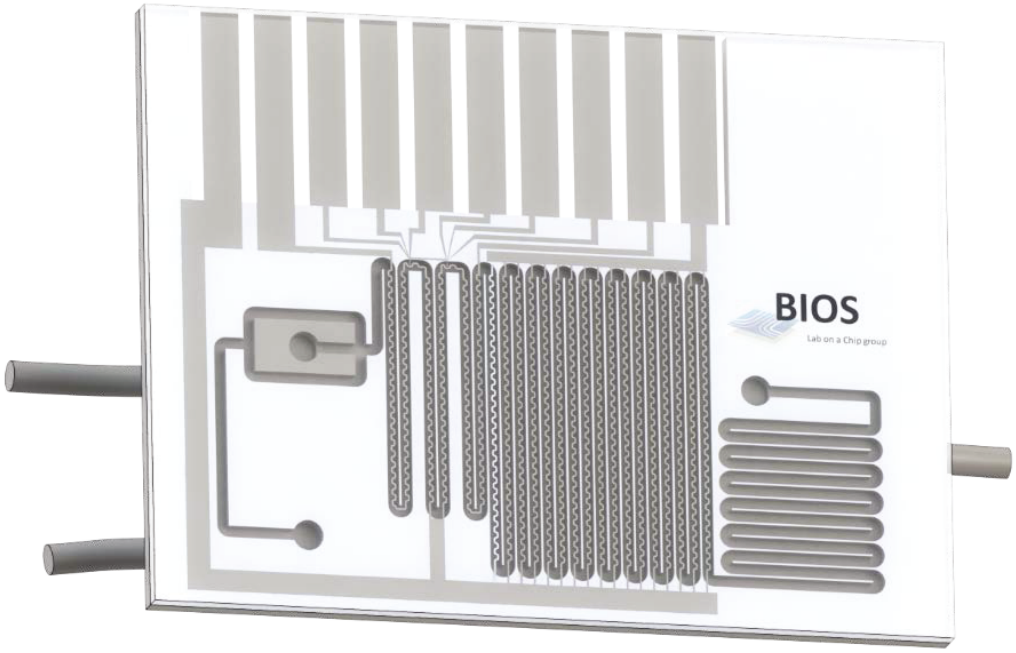

UNIVERSITY OF TWENTE
MCEC PROGRAM
EWI
BIOS-LAB-ON-A-CHIP GROUP
MASTER ELECTRICAL ENGINEERING
TIME AND DATE: 15h, 1 July 2016
REPORT NO.: 2016-17

EXAM COMMITTEE:
Prof.dr.ir. A. van den Berg
Dr.ir. M. Odijk
Dr.ir. R.M. Tiggelaar
Prof.dr. J.G.E. Gardeniers
Prof.dr.ir. B.M. Weckhuysen

INTRODUCTION AND OUTLINE

For my master thesis at the BIOS-Lab-on-a-Chip group, and as a part of the Netherlands Centre for Multiscale Catalytic Energy Conversion (MCEC) program, I was tasked with the assignment of designing and testing a 'Single Catalyst Particle Diagnostics: Droplet Microreactor platform'. This microreactor should be able to study single catalyst particles at high temperatures. As a report I have written a paper entitled *'Design and characterization of a microreactor for monodisperse catalytic droplet generation at elevated temperatures and/or pressures'*. In this paper I will explain all the results and findings obtained so far. The title is slightly different from the title chosen for my thesis, because the actual diagnostics within a droplet have not been achieved yet. However, as I will demonstrate, a microreactor with the potential of doing exactly that has been fabricated. The paper is accompanied by a supplementary information with more details about certain design aspects mentioned in the paper. As a small background the official project description from the MCEC website is given, followed by the paper and supplementary information.

BACKGROUND

Recent studies indicate that heterogeneous catalysts vary tremendously, induced by dynamic changes in active sites both between and within single catalyst particles. Traditional characterization approaches of catalyst particles in large reactor vessels results in measurements representing ensemble averages. On the other hand, individual particle characterization is costly and time consuming and can therefore only be done on a limited amount of catalyst particles. There is a need for a single catalyst diagnostic platform to characterize single particles at low-cost and high-throughput, to enable a massive search to find and select the best catalyst particles and related synthesis formulation approaches. Droplet microfluidics can trap single catalyst particles at several thousands of droplets per second, and allows to graft, react, and analyse each particle individually. The most promising particles can be selected for further in-depth analysis. Ultimately, the knowledge obtained from this research project will help to improve catalyst particles for use in fluid catalytic cracking (FCC) in the areas of the petrochemical industry and biomass conversion[1].

[1] The background description is taken from the MCEC website: http://www.mcec-researchcenter.nl/projects/single-catalyst-particle-diagnostics-droplet-microreactor-platform/

Design and characterization of a microreactor for monodisperse catalytic droplet generation at elevated temperatures and/or pressures

J. C. Vollenbroek[a], A. E. Nieuwelink[b], J. G. Bomer[a], R. M. Tiggelaar[c], A. van den Berg[a], B. M. Weckhuysen[b], M. Odijk[a]

Catalyst particles used in the Fluid Catalytic Cracking (FCC) of crude oil show large variations in activity both between and within particles . This paper reports the results of the fabrication and characterization of a microfluidic droplet microreactor with potential usfor single catalyst particle diagnostics. The microreactor features a droplet generator, microheaters, micro temperature sensors, and is able to operate at pressures up to 5 bar as of now. This microreactor consists of fluidic channels etched in a silicon wafer and platinum heater and sensor structures embedded in the glass cover. Temperature characterization showed linear behaviour of the sensors with respect tot temperature, with a resolution of 0.15 ℃, and a sensitivity of 0.0476 $\Omega°C^{-1}$. Furthermore, a PI controller allows control of the heaters within 2.6 ℃ of the desired temperature. Highly stable and monodisperse oil-in-water droplets are created and heated up to 100 ℃ at atmospheric pressure, and up to 120 ℃ at an outlet backing pressure of 5 bar. Preliminary results on the fluorescent detection of the oligomerization reaction of 4-fluorostyrene with zeolite H-ZSM-5 shows the potential of the microreactor chip in investigating the catalytic activity and efficiency of FCC particles.

1.INTRODUCTION

Recent studies show that the particles used in the Fluid Catalytic Cracking (FCC) of crude oil show significant variations in activity both between and within particles [1,2]. These heterogeneous catalysts are under a lot of stress during the cracking process. Metal poisoning and coke formation are examples of contamination that impair the efficacy of a FCC particle [1]. Characterization of the particles is done in large reactors from which only ensemble averages are obtained. So far, the analysis of a single particle is both time consuming and costly [1]. In this paper we present a microfluidic platform dedicated to single catalyst particle diagnostics, consisting out of a droplet generator, which can create up to thousands of droplets per second, and a microheater. Inside the droplet, the activity of a single particle can be studied using fluorescence microscopy.

FCC particles are a combination of several materials including clay, zeolite, alumina, and silica. The particle is porous and the pore size decreases towards the centre of the particle. As the oil chain is being cracked when moving into the particle, the smaller components can penetrate deeper into the particle [1]. The cracking of oil takes place at both Lewis and Brønsted acid sites inside the FCC particle. A Brønsted acid site is a solid acid, occurring at places where an aluminium atom is embedded into the silicon lattice, and can attract a proton. Studies have shown that the zeolite inside the FCC particle contains the most solid acid sites, thus being the main active component in the cracking of oil [1–3]. There are several zeolites and from research it is known that its active sites can be studied by either UV-vis spectroscopy [2] or fluorescence microscopy [4]. In both cases an oligomerization reaction of styrene, catalysed by the solid acid sites found in zeolites, is studied. Stavitski et al. 2009 [4], show different styrene additives and the fluorescent intensities that were measured after the reaction of the styrene additives with zeolite H-ZSM-5. The aforementioned reaction takes place between 100 – 200 ℃ and took about 5 minutes to complete.

In the field of microfluidics the use of microdroplets is common practice. Microdroplets are used in many applications such as chemical microreactors and single particle traps to biological assays of cells and DNA [5–8]. By mixing two immiscible fluids such as oily (nonpolar) and watery (polar) substances, either oil in water (O/W) or water in oil (W/O) droplets are created [5,6,9]. A droplet is the result of the shear forces and interfacial tension between the two fluids, creating a stream of liquid A (continuous phase) with droplet of liquid B (dispersed phase) [6]. It is important that the walls of the channel have a preference to be wetted by the opposite phase than that of the droplet, as is demonstrated in [9]. Droplets form an ideal reaction environment because of their well-controlled properties such as shape, size, and monodispersity, creating a homogeneous reaction environment. The configuration of the channels that are used for the creation of droplets also plays a role. Examples of geometry types are the Capillary, the T-junction, and the Flow Focusing junction [6].

To achieve the temperature range in which the reactions with styrene occur, thin film platinum structures that can be heated via joule heating are incorporated on the chip. These platinum heaters are stable up to at least 500 ℃ [10,11], depending on the adhesion layer that is used. These thin film microheaters have been used a lot in literature [10,11,13–22]. Varying from use in biological assays [16-18,20,21], to reactors or hotplates for single phase purposes [11,13,14,19], and finally to reactions inside droplets on a microfluidic chip [12,17]. In these last two cases this was either done in stationary droplets [17], or with bulky heating systems [12]. The ability to use microfluidic systems at elevated pressures has been demonstrated previously [23,24], where the possibility of both high pressure and high temperature is reported in [23].

Although heterogeneous catalysis has been performed before in droplets on a millifluidic chip [12], this has not been done with an integrated heater section, but in an oven. Other work in microreactors was either not in droplets [11,13,14,19], or if they were, in bulky systems [12], and with stationary droplets [17]. This single catalyst particle diagnostic platform is designed to measure the activity of FCC particles and offers a well-

controlled reaction environment with respect to both volume and temperature; all features integrated into a single microfluidic chip, and without large control systems. The throughput is in theory limited by the optical detection method and the reaction time.

2. DESIGN & SIMULATION

2.1 Design considerations

The chip in Figure 1 (A) shows the design of the microreactor. It has several features, including a droplet generator (C), microreactor (B), and temperature sensor section (D). As the main geometry for creating droplets, the flow focusing junction was chosen for stability reasons. Oil flows in the main channel via inlet I2, and water through the sides via inlet I1 to create droplets of oil in water. The heater section contains three separate heaters. Heater 1 and heater 2 (H1 and H2) can be controlled separately via electrodes E9 and E2. Both these heaters have an interwoven temperature sensor, so they can be monitored and controlled via software. These temperature sensors can be seen in Figure 1 C. A four point measurement, in which a current is steered through electrode E3 and E8, creating a voltage drop over the small resistor structure, is used to measure the resistance of the sensor. The voltage can be measured between electrodes E4 and E5, and electrodes E6 and E7. When the temperature increases, the resistance increases resulting in an increasing voltage across the aforementioned electrodes. The final heater section, H3, is a block of parallel heaters. These heaters have no dedicated temperature sensor. The parallel heaters are connected to E10; E1 is the ground electrode to which all heaters are connected. When H1 and H2 are at the desired temperature, the power used for heating is calculated and with that the power for H3 can be proportionally estimated via software. The parallel heater section, as well as the meandering structure of the channels, are necessary to give the reaction enough time to occur at elevated temperatures. This standard design has some variations. The channel width varies between 150 – 300 μm, with steps of 50 μm. For some chips a T-junction is used as the droplet generator, and finally the area that is covered by the parallel heater is varied between different chips. The chip as a whole is 15mmx20mmx1mm.

2.2 Simulation

For an estimation of the amount of power that is needed to heat up the fluids in the channel, a COMSOL simulation has been performed. Figure 2 shows the geometry of the device. Because of the symmetry of both heater and channel, only half of the channel is simulated[1]. All surfaces marked with an 'S' are the symmetry planes of the simplified model. Further included in the geometry are the silicon substrate (3), the fluid (water) present in the channel (2) and the platinum heating filament (1). The insulating SiO_2 layer on the channel wall has been left out because calculations[1] showed that the transition between silicon and air was the largest thermal barrier i.e. the highest thermal resistance.

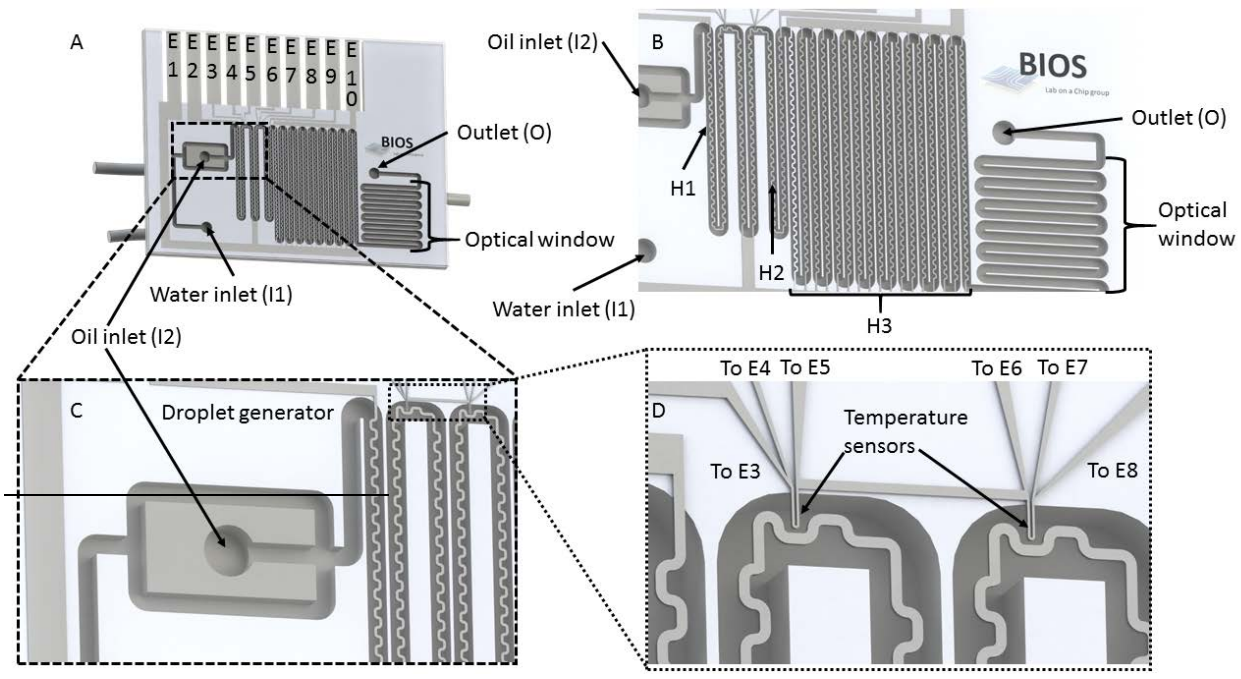

Figure 1: Overview of the microreactor chip design. Channels have a height and depth of 150 micron, heaters are 45 micron wide and 200 nm thick, and the temperature sensor has a width of 10 micron and thickness of 200 nm. All heater related structures are made out of platinum, the bottom substrate is silicon and the top substrate is glass. Furthermore, the picture contains images of A) broad overview showing the electrodes (E1-E10), channel layout, inlets for the dispersed phase (I1) and continuous phase (I2), and the outlet (O). B) Close up of the heater sections showing the three different heaters (H1 – H3) that can be controlled via electrodes E2 (H1), E9 (H2), and E10 (H3). C) Close up of the droplet generator feature, showing the flow focusing junction and the inlet for the dispersed phase. D) Close up of the temperature sensor structure combined with the electrodes used for addressing them.

[1] For reasoning and motivation about geometry, calculations, and simplification decisions in the simulations, Supplementary Information (SI.1) should be consulted.

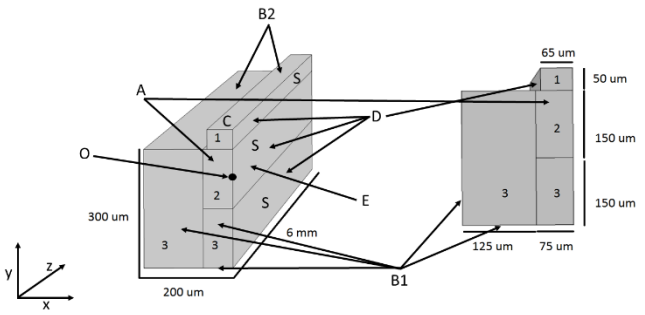

Figure 2: Geometry used in the COMSOL simulation showing materials, dimensions, and boundary conditions that are used. Materials being platinum (1), water (2), and silicon (3). Boundary conditions are: Inlet parabolic velocity profile for the fluidic channel (A), heat loss modelled as an outflux of 953 $\mathrm{Wm^{-2}K^{-1}}$ (B1) and 10 $\mathrm{Wm^{-2}K^{-1}}$ (B2), Heat source of 300 mW (C), Thermally insulating surfaces (D), and no viscous stress (E) on the appointed channel wall. (O) marks the origin of the channel. (S) marks the symmetry plane of the geometry.

In the simulation the heat transfer module, laminar flow model, and Multiphysics for non-isothermal flow, are used. The formula for the stationary heat equation is given below in equation (1) and (2)

$$\rho C_p \mathbf{u} \cdot \nabla T + \nabla \cdot \mathbf{q} = Q \quad (1)$$

$$\mathbf{q} = -k\nabla T \quad (2)$$

Where ρ is the density in $\mathrm{kgm^{-3}}$, C_p is the heat capacity at constant pressure in $\mathrm{Jkg^{-1}K^{-1}}$, T is the temperature in K, q is the heat flux in $\mathrm{Wm^{-2}}$**,** Q is the volumetric heat flux in $\mathrm{Wm^{-3}}$ and u is the velocity vector in $\mathrm{ms^{-1}}$. Note that bold variables/parameters **u** and **q** are vectors and other variables/parameters are scalars or mathematical operators. For the laminar flow domain, a parabolic flow profile is present at the inlet. The formula used for the determination of the laminar flow profile is given in equation (3) taken from [25].

$$v_z = \frac{9}{4}\frac{Q_f}{HW}\left(1 - 4\left(\frac{y_0+\Delta y}{H}\right)^2\right)\left(1 - 4\left(\frac{x_0+\Delta x}{W}\right)^2\right) \quad (3)$$

Where v_z is the velocity in the z-direction in $\mathrm{ms^{-1}}$, H is the height of the channel in m, W is the width of the channel in m, y_0 and z_0 are at the origin of the channel, which indicated with an 'O' in Figure 2, Q_f is the flow rate in $\mathrm{m^3s^{-1}}$. The walls of the channel were given no slip condition, meaning that v = 0 at the walls. Boundary conditions used in the simulation are listed below and clarified in Figure 2.

Inlet velocity profile (A): Equation (3) was given as a formula for the velocity profile of the flow.

Heat flux condition (B1 and B2): The heat flux is the outflow of heat normal to the surface area. The convective heat flux is given by: $q_0 = h(T_{ext} - T)$, where h is the heat transfer coefficient in $\mathrm{Wm^{-2}K^{-1}}$, T_{ext} and T are the temperatures outside and inside the device in K. Calculations gave an estimation for the heat loss as if the simulated geometry were the size of the design, resulting in a heat transfer coefficient of 953 $\mathrm{Wm^{-2}K^{-1}}$ for surfaces marked by B1, and a smaller heat transfer coefficient for surfaces in normal contact with air, B2, with a heat transfer coefficient of 10 $\mathrm{Wm^{-2}K^{-1}}$.

Heat source (C): The platinum element is modelled as a heat source with an empirically determined power of 300 mW.

Thermally insulating (D): The symmetry plane and the sides of the heater were made thermally insulating.

No viscous stress (E): The symmetry surface of the channel is given a no viscous stress condition, to allow the fluid to have a velocity at this surface, therefore create half of a parabolic flow profile[2].

Material properties and parameters used in the simulation are listed in Table 1. The simulation result shows a cross-section of the channel and the corresponding temperature profile inside the channel, as shown in Figure 3. Because the temperature is uniform (Uniformity is shown in Supplementary Information SI.1) along the length of the channel, this can be at any point on the z-axis. This temperature is in the range of the temperature needed for the reaction. With this result the power per unit area for the platinum heat source in the simulation was related to the total contact area between the heaters and the channel in the design. This leads to an estimated power of 1.13 W.

Table 1: Parameters for the different materials used in the calculation of the heat transfer coefficient of the microreactor

	Thermal conductivity ($\mathbf{Wm^{-1}K^{-1}}$)	**Density ($\mathbf{kgm^{-3}}$)**	**Heat transfer coefficient ($\mathbf{Wm^{-2}K^{-1}}$)**	**Thermal capacity ($\mathbf{Jkg^{-1}K^{-1}}$)**
Water	0.6	1	N.A.	4185.5
Si	130	2329	N.A.	700
Platinum	71.6	21450	N.A.	133
Air	N.A.	N.A.	10	N.A.

[2] In Supplementary Information (SI.1) more about the exact shape of this "half" parabolic flow profile is given.

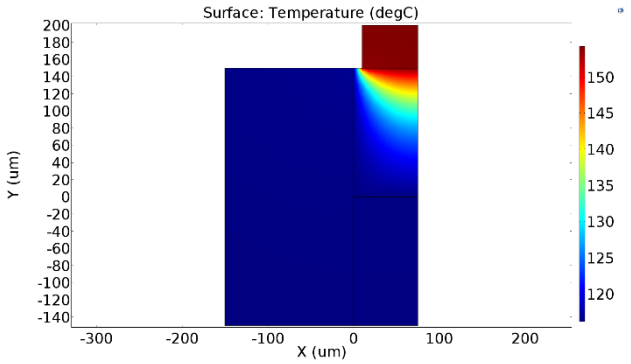

Figure 3: Cross-sectional image of the channel with heater element. The image shows the temperature distribution within the channel The power applied to the heater during the simulation was 300 mW. Image taken at z = 200 µm

3. EXPERIMENTAL

3.1 Fabrication

The chips were fabricated in cleanroom of the MESA+ NanoLab at the University of Twente. Figure 4 shows an overview of the process steps that were done to fabricate the chip. Supplementary Information (SI.2) provides more information about the masks that were used during the processing. The chip is a stack of a silicon and a glass substrate bonded together. A three mask process is used to develop the desired features in/on both substrates, as shown in Figure 4. Using photolithography with mask 1, the pattern for the platinum structures is created on a glass substrate. With BHF as a wet etchant the pattern is etched 200 nm deep into the glass substrate. This process is directly followed by the deposition of a 10 nm thick tantalum adhesion layer and a 190 nm thick platinum layer, causing the heater to be embedded into the glass substrate. After this the complete glass substrate is covered with 1 µm PECVD SiO2 and mask 3 is used to remove this SiO2 layer from the contact electrodes and at the fluidic accesses. Mask 2 is then used to create the channel pattern on the silicon substrate. The channels are made 150 µm deep using DRIE etching. With mask 3 the pattern for the contact holes and fluidic accesses was made on the backside of the silicon substrate; this time DRIE etching is used to etch all the way through the silicon. This ensures the accessibility of the electrodes and channels when the substrates are bonded together. Before that final step the silicon substrate is first put into the oven for dry oxidation of Si. This creates the 200 nm thin insulating SiO_2 film on the walls of the channel. Post to completion of all process steps, the silicon and glass substrates are anodically bonded, and the individual chips released by dicing.

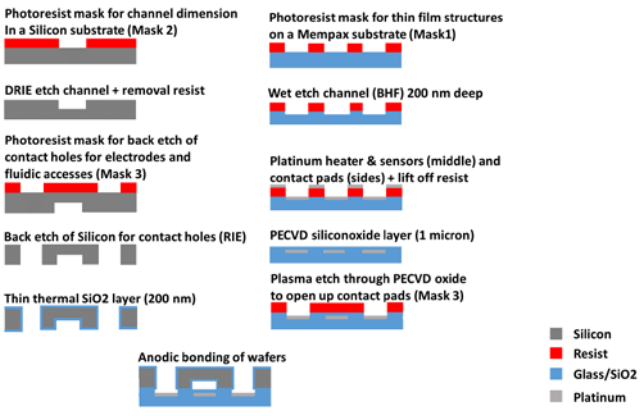

Figure 4: Side view of the different steps used in the process of fabrication of the droplet microreactor.

3.2 Temperature sensor characterization

Characterization of the temperature sensors is done by mounting the chip on a Princted Circuit Board (PCB) and wirebonding the electrodes to the PCB, so the chip can be addressed via external connectors. The chip is fully immersed in a beaker of oil standing on a hotplate, type IKA RET. A thermocouple thermometer, connected with the hotplate, is used as a reference thermometer and measures the temperature of the oil. A magnetic stirring bead is added to increase the uniformity of the temperature in the oil. The hotplate is heated from 30 °C to 150 °C and back, to rule out any hysteresis effects. Meanwhile the resistance of the temperature sensor on the microreactor is measured. A signal from the sensor is measured by steering a current through it, using a LM317TG voltage regulator as current source. The voltage occurring across the resistor is amplified using a AD620ANZ instrumentation amplifier. The output signal is recorded by a NI myRio connected with Labview software on the computer. Supplementary Information (SI.3) provides more information about read-out electronics.

3.3 Chipholder and control of the heaters

For control of the heaters, the chip is placed into a Delrin chipholder, chosen for its low thermal conductivity. This chipholder consists of a bottom and top part. For control of the heaters a PI controller is made in Labview and executed on the NI myRIO. The PI controls the duty cycle of a 1000 kHz square wave put onto the gate of a NMOS transistor FDN5630. The NMOS acts as a switch between a 48V power source and the heaters. By varying the duty cycle the power to the heaters can be controlled. The temperature sensors in the microreactor chip provide the feedback temperature for the control loop. Supplementary Information (SI.3) provides more information about the control.

3.4 Droplet creation

Droplets are created by connecting a Nemesys syringe pump, with Hamilton syringes of 500 µL (oil) and 1000 µL (water), Fused silica tubing (Polymicro Technologies, ID = 100 µm, OD = 360 µm), to the oil and water inlets of the microreactor. The pump is controlled with Nemesys software. For the dispersed phase FC-40 oil is used and for the continuous phase MilliQ demiwater. A CCD high speed camera and FPV software, in combination with a Leica DMi 5000 M microscope is used to capture movies and images from the droplets whilst created. Experiments at high pressure can be done by adding a backpressure regulator, P786 from idex-hs, with a backing pressure of 5 bar.

3.5 High temperature reactions inside droplets

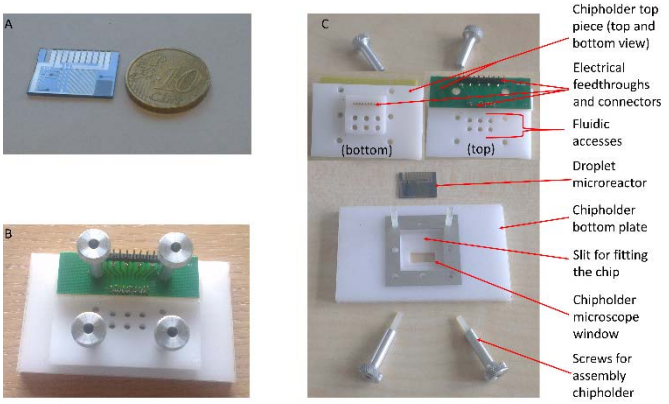

Figure 5: Chip and chipholder assembly showing A) the droplet microreactor chip, B) the chipholder fully assembled, and C) an exploded view of the chipholder with chip showing the different part from top to bottom: Top piece of the chipholder, electrical feedthroughs necessary to address the chip electronically, fluidic contact holes used for connecting fluidic tubing, the droplet microreactor chip, the bottomplate of the chipholder, the slit were the chip fits into the holder, the window through which the chip can be studied with a microscope, and finally the screws for holding together the whole assembly.

For proof of principle testing, an oligomerization reaction with zeolite H-ZSM-5 powder and 4-fluorostyrene, suspended in hexadecane (all from Sigma Aldrich), is done inside the microreactor chip. This reaction, previously done by Aramburo et al 2012 [3], is illustrated in Scheme 1. Aforementiond reaction does not take place at room temperature and starts up slowly at 80 ℃ [4].The reaction products, shown in Scheme 1, are a linear dimeric carbocation (D) and a cyclic dimeric species (E), having an absorption band at 520 nm and 565 nm respectively [3]. Fluorescence images are made of the inside of the channels of the microreactor at room temperature and at 140 ℃. The excitation wavelength of the laser that is used is 561 nm and the emission of the sample is 605 nm. Images are captured with a Nikon Eclipse confocal fluorescence microscope.

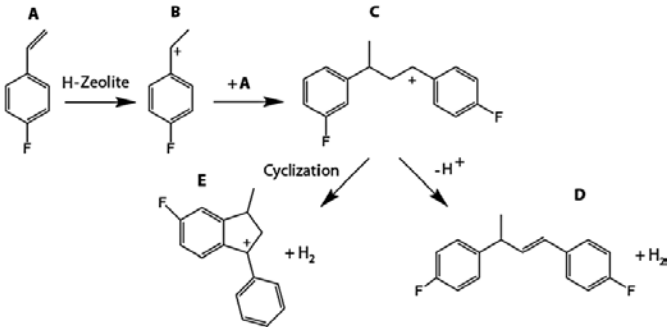

Scheme 1: Competitive reaction pathways in the Brønsted acid-catalyzed oligomerization of 4-fluorostyrene on H-ZSM-5 zeolites. The initial benzylic carbocation (B) is formed due to the protonation of the styrene derivative by a Brønsted acid site. Dimerization with another 4-fluorostyrene monomer (A) gives rise to the linear dimeric 1,3-bis(4-fluorophenyl)-1-butylium cation (C). This carbocation can be transformed either into 3-methyl-1,4-fluorophenylindranyl (E) by acyclization reaction or into a conjugated linear dimeric 1,3-bis(4-fluoro-phenyl)-2-buten-1-ylium carbocation (D). Scheme is taken from [3]

4. RESULTS

4.1 Temperature sensor characterization

Successful fabrication resulted in the chip shown in Figure 6. Showing all features like, the droplet generator, heaters (H1, H2, and H3), temperature sensors, inlets (oil and water), outlet, and the optical window, as mentioned in section 2.1 regarding the design. Created channels are 150 µm deep. Temperature characterization is performed using the oil immersion method as described in the experimental section. The results are shown, for the sensor (S1) at H1 only, in Figure 7. The graph for the other sensor (S2) can be found in Supplementary information (SI.4). The temperature characteristic of the sensors is highly linear, given the R^2 of 0.99899 for S1 and an R^2 of 0.9989 for S2. The sensitivity for both sensors is 0.0476 $\Omega°C^{-1}$, and the offsets are 18.311 Ω and 18.294 Ω for S1 and S2 respectively. Because of the uniformity, this characteristic is used for all the sensor structures made on the same wafer, since they were made in the same process. From this characteristic also the resistivity and temperature coefficient of resistance (TCR) for the platinum layer is calculated, being 1.6667e-07 Ωm and 0.0025 $°C^{-1}$ respectively. The resolution of the temperature sensors is 0.15 °C, determined by the 12 bit ADC and gain of the electric circuit amplifying the voltage across S1 and S2. More information regarding the read-out circuit can be found in Supplementary Information (SI.3).

4.2.1 Control of the heaters H1 and H2

Testing the control of the heater is done by varying the setpoint of the PI control described in section 3.3. The setpoint of the control loop is varied between 23°C and 120 °C; during these experiments droplets were created at the same time inside the microreactor chip. It can clearly be seen that when the setpoint is increased form 50 °C to 75 °C, the duty cycle increases immediately, resulting in an increased power dissipation, and therefore increased temperature of the heater. The step response time (time needed to reacht the setpoint) is approximately 1.5 seconds after which the temperature oscillates around the setpoint. There is a standard deviation of 2.6 °C around the setpoint and calculations shows that 530 mW is needed to reach 50 °C. More information about the control measurements regarding H1 and H2, and the calculated values above, can be found in Supplementary Information (SI.4) .

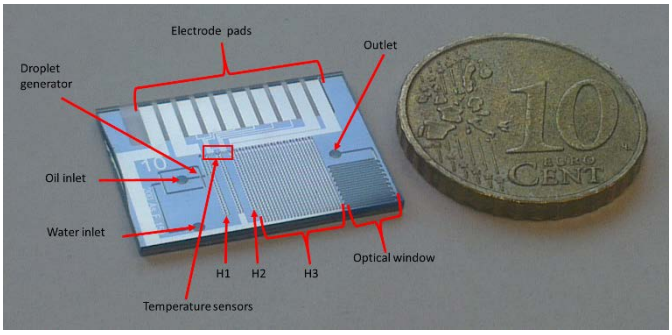

Figure 6: Fabrication result of the droplet microreactor chip. Image shows the different features also highlighted in the design in Figure 1.

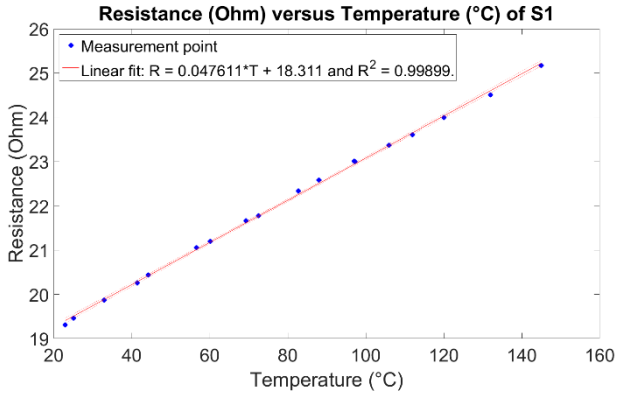

Figure 8: Change in resistance with respect to temperature of sensor S1.

4.2.2 Use of the parallel heaters

The parallel heaters (H3) can be manually controlled via the Labview software. They are connected to a different NMOS than H1 and H2. The parallel heaters generate enough heat to be measured by S1 and S2. By carefully adjusting the duty cycle of H3, it can be optimally tuned for assisting H1 and H2. More information about the control measurements regarding H3 can be found in Supplementary Information (SI.4).

4.3 Droplets at different temperatures and pressure

Droplets were created using the setup described in section 3.4. Several tests were done with droplets being created in various conditions, as shown in Figure 8, where A) the heaters are switched off, B) the temperature is kept at 50 °C and C) 75 °C, D) the temperature is above the boiling point of water (120°C), and finally E) the temperature is above the boiling point of water (120 °C), but the system is under an outlet pressure of 5 bar approximately. For all measurements the flow rates of the water and oil phase are 15 $\mu L/min$ and 3 $\mu L/min$ respectively, and images were taken by the high-speed camera with a framerate of 125 fps. The width of the channel is these measurements was 250 μm. Figure 8 A) shows the image of droplets created at room temperature. The created droplets are highly monodisperse, as shown in Figure 8 B) and C), where droplets at 50 °C and at 75 °C are depicted. The volume of the droplet is approximately 47 nL and the and does not change with temperature. The volume was determined by using height and width of the channel and the length of the heater filament covered by the droplet. A measurement with a different chip at different flowrates is shown in Supplementary Information (SI.5) to provide more data on monodispersity and droplet volume. When the temperature is increased to 100 °C, small gas bubbles start to appear in the channel. The bubbles find their origin under the heater and when they encounter an oil droplet they show affinity towards the oil phase. Inside the oil bubble the small bubbles seem to follow the path of the heater. Figure 9 illustrates the appearance of gas bubbles, their accumulation in the oil droplet, and their behaviour in following the heater trace. At 120 °C large gas bubbles are formed and the droplets start to fall apart, showing dewetting phenomenon at the channel ceiling surface. A collapsed droplet, with large gas bubbles in the droplet, is shown in Figure 8 D) . When the backpressure regulator is added, the droplets are still intact at 120 °C. This is shown in Figure 8 E). The monodispersity is warranted when working above atmospheric pressure at the outlet.

4.4 Reaction in single phase flow

In order to observe the influence of temperature on the reaction, first a control measurement is done. For this control measurement, the H-ZSM-5 with 4-fluorostyrene and hexadecane mixture is flushed through the chip with the heaters off. A flow rate of 3 $\mu L/min$ is used. The fluorescence image shown in Figure 10 A) is taken at a spot in the channel, at room temperature. The heaters are then set at a temperature of 140 °C and a fluorescence image is taken from the same part of the channel. These figures show that there is a small change in fluorescence signal for this particular area when the heaters are switched on, with respect to when they are switched off.

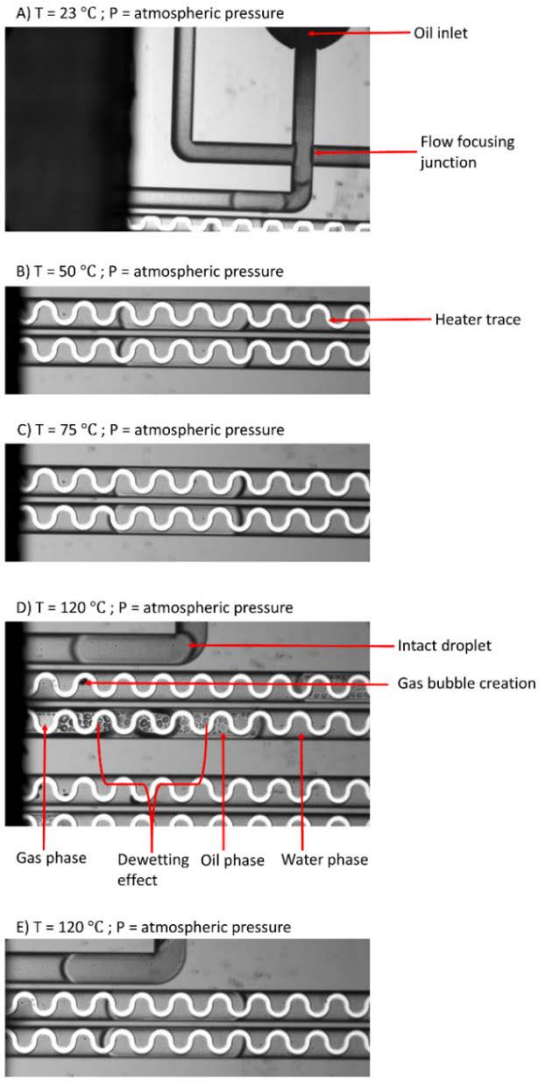

Figure 7: Droplets created under various conditions, where at A) the heaters are switched off, B) the temperature is kept at 50 °C and C) 75 °C, D) the temperature is above the boiling point of water (120°C), and finally E) the temperature is above the boiling point of water (120 °C), but the system is under an outlet pressure of 5 bar approximately.

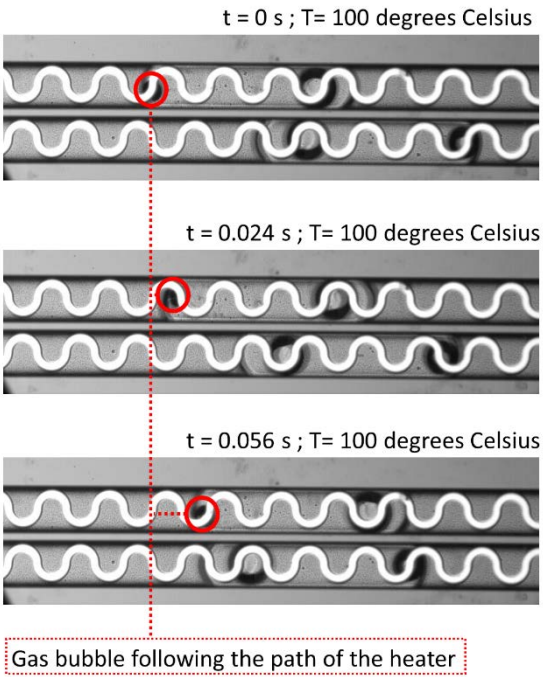

Figure 10: Gas bubbles following the trail of the heater when the temperature is close to the boiling point of water (100 °C). The three images above show three different stages in time where the bubble changes position with respect to the width of the channel. The change corresponds with the path of the heater.

Upon completion of the measurement other areas of the chip were inspected and a large agglomeration of particles near the inlet was observed. Apparently, the zeolite particles attached to the wall, as shown in Figure 10 B). These fluorescent parts around the inlet could not be flushed out of the channel, even with high flow rates up to 120 $\mu L/min$.

5. Conclusion and outlook

Successful creation of droplets, as well as heating the droplet under high pressure has been achieved with the droplet microreactor. Fabrication of the microreactor has been achieved with a three mask process. Preliminary results show proof of principle, in a one phase flow, by the oligomerization reaction of 4-fluorostyrene with zeolite H-ZSM-5 at 140 °C, whereas the reaction does not occur at room temperature. Generated droplets are highly monodisperse, creating well defined and uniform reaction environments. The temperature of the heater elements can be controlled with a standard deviation of approximately 2.6 °C from the setpoint. Measurment of the temperature can be done with a resolution of 0.15 °C The appearance of gas bubbles inside stable oil droplets around 100 °C gives the opportunity to study reactions with gas on the chip in a three phase system.

As of now, the proof of principle reaction has been done in a one phase flow. In order to get more elaborate and conclusive proof about the ability to do controlled reactions on the chip, the reaction needs to be done in an actual droplet. This can give more insight to the reaction rates when the fluorescent intensity is measured as the droplet travels along the channel. Furthermore, instead of zeolite powder, the real FCC particles should be tested. To do this, the particles must be captured in droplets first. This might cause problems, because it is known that FCC particles sink quickly, and thus do not stay in suspension. Upon achievement of FCC particle encapsulation their activity and behaviour can be studied on chip. Finally, the temperature inside the channel needs to be calibrated, since the temperature read-out from the platinum sensors solely contains information about the temperature on the surface of the channel, on only two places. In collaboration with Utrecht University, luminescent nanoparticles can be used to map the temperature inside channels [26], as well as the temperature distribution over the chip as a whole.

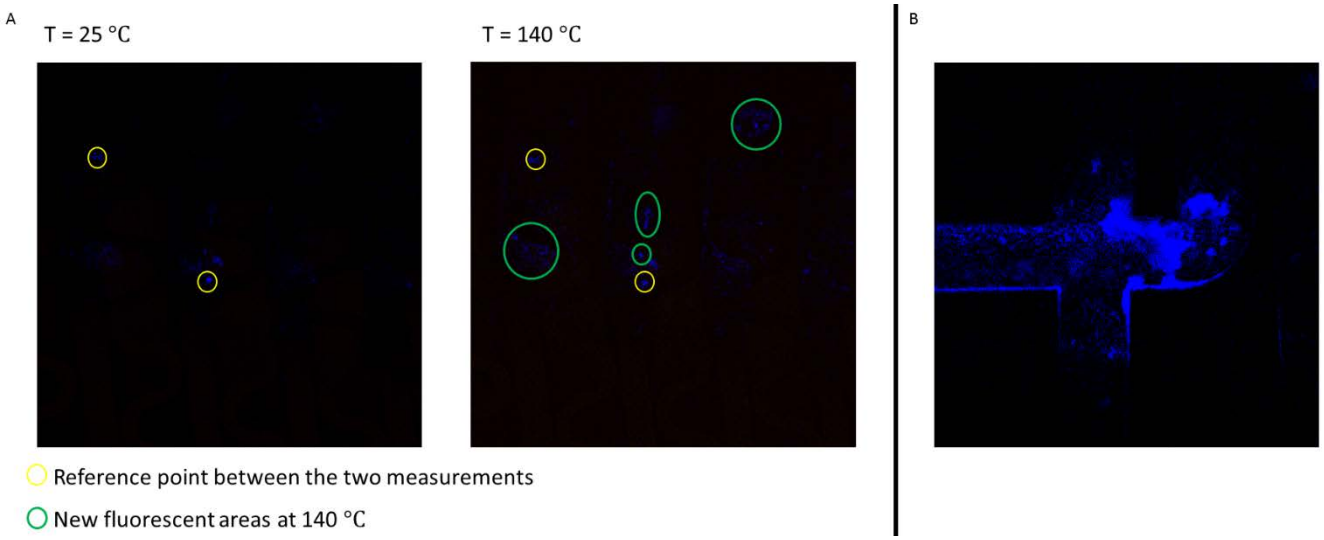

Figure 9: Reaction of 4-fluorostyrene with zeolite H-ZSM-5 made visible by fluorescence microscopy. With A) a fluorescent image at the same spot in the channel at different temperatures (25 °C and 140 °C), where the fluorescent signal increased when the heaters were switched on. B) fluorescence image of the inlet after completion of the experiments, showing that the amount of heat produced in the chip was enough to get the reaction going near the inlet. Please note that the images in A) have been treated using adobe Photoshop. The exposure of the images was raised from 0 to +3.8 in order to enhance the contrast between the fluorescent signal and the background.

Acknowledgements

This work was supported by the Netherlands Center for Multiscale Catalytic Energy Conversion (MCEC), an NWO Gravitation programme funded by the Ministry of Education, Culture and Science of the government of the Netherlands. Further gratitude is reserved for S. Dekker, H. de Boer, C. Bruinink for helping with fabrication of both chip and chipholders. M. Welleweerd is thanked for his expertise in Solidworks and Photoshop.

J. C. Vollenbroek,[a] A. E. Nieuwelink[b], J. G. Bomer[a], R. M. Tiggelaar[c], A. van den Berg[a] , B. M. Weckhuysen[b] , M. Odijk[a]

[a] BIOS Lab-on-a-Chip Group, MESA+ Institute for Nanotechnology, MIRA Institute for Biomedical Technology and Technical Medicine, University of Twente.

[b] Inorganic Chemistry and Catalysis, Debye Institute of Nanomaterials Science, Utrecht University.

[c] NanoLab cleanroom, MESA+ Institute for Nanotechnology, University of Twente.

Notes and references

[1] E.T.C. Vogt, B.M. Weckhuysen, Fluid catalytic cracking: recent developments on the grand old lady of zeolite catalysis, Chem. Soc. Rev. 44 (2015) 7342–7370. doi:10.1039/C5CS00376H.

[2] I.L.C. Buurmans, J. Ruiz-Martínez, W. V. Knowles, D. van der Beek, J. a. Bergwerff, E.T.C. Vogt, et al., Catalytic activity in individual cracking catalyst particles imaged throughout different life stages by selective staining, Nat. Chem. 3 (2011) 862–867. doi:10.1038/nchem.1148.

[3] L.R. Aramburo, S. Wirick, P.S. Miedema, I.L.C. Buurmans, F.M.F. de Groot, B.M. Weckhuysen, Styrene oligomerization as a molecular probe reaction for Brønsted acidity at the nanoscale, Phys. Chem. Chem. Phys. 14 (2012) 6967. doi:10.1039/c2cp22848c.

[4] E. Stavitski, M.H.F. Kox, B.M. Weckhuysen, Revealing shape selectivity and catalytic activity trends within the pores of H-ZSM-5 crystals by time- and space-resolved optical and fluorescence microspectroscopy, Chem. - A Eur. J. 13 (2007) 7057–7065. doi:10.1002/chem.200700568.

[5] S. Teh, R. Lin, L. Hung, A.P. Lee, Droplet microfluidics., Lab Chip. 8 (2008) 198–220. doi:10.1039/b715524g.

[6] X. Casadevall i Solvas, A. DeMello, Droplet microfluidics: recent developments and future applications., Chem. Commun. (Camb). 47 (2011) 1936–42. doi:10.1039/c0cc02474k.

[7] J.H. Leamon, D.R. Link, M. Egholm, J.M. Rothberg, Overview: methods and applications for droplet compartmentalization of biology., Nat. Methods. 3 (2006) 541–543. doi:10.1038/nmeth0706-541.

[8] R.M. Schoeman, Droplet Microfluidic Platform for Cell Electrofusion, University of Twente, 2015. doi:13.3990/1.9789036539548.

[9] L. Shui, A. van den Berg, J.C.T. Eijkel, Interfacial tension controlled W/O and O/W 2-phase flows in microchannel., Lab Chip. 9 (2009) 795–801. doi:10.1039/b813724b.

[10] R.M. Tiggelaar, R.G.P. Sanders, A.W. Groenland, J.G.E. Gardeniers, Sensors and Actuators A : Physical Stability of thin platinum films implemented in high-temperature microdevices, 152 (2009) 39–47. doi:10.1016/j.sna.2009.03.017.

[11] W. Chang, Y. Hsihe, Microelectronic Engineering Multilayer microheater based on glass substrate using MEMS technology, MEE. 149 (2016) 25–30. doi:10.1016/j.mee.2015.09.005.

[12] K. Olivon, F. Sarrazin, Heterogeneous reaction with solid catalyst in droplet-flow millifluidic device, Chem. Eng. J. 227 (2013) 97–102. doi:10.1016/j.cej.2012.08.098.

[13] R.M. Tiggelaar, P. Van Male, J.W. Berenschot, J.G.E. Gardeniers, R.E. Oosterbroek, M.H.J.M. De Croon, et al., Fabrication of a high-temperature microreactor with integrated heater and sensor patterns on an ultrathin silicon membrane, 119 (2005) 196–205. doi:10.1016/j.sna.2004.09.004.

[14] R.M. Tiggelaar, P.W.H. Loeters, P. Van Male, R.E. Oosterbroek, J.G.E. Gardeniers, M.H.J.M. De Croon, et al., Thermal and mechanical analysis of a microreactor for high temperature catalytic gas phase reactions, 112 (2004) 267–277. doi:10.1016/j.sna.2004.01.036.

[15] V. Miralles, A. Huerre, F. Malloggi, M. Jullien, A Review of Heating and Temperature Control in Microfluidic Systems: Techniques and Applications, 2013. doi:10.3390/diagnostics3010033.

[16] J.L. Lin, M.H. Wu, C.Y. Kuo, K. Da Lee, Y.L. Shen, Application of indium tin oxide (ITO)-based microheater chip with uniform thermal distribution for perfusion cell culture outside a cell incubator, Biomed. Microdevices. 12 (2010) 389–398. doi:10.1007/s10544-010-9395-4.

[17] C. Fang, D. Lee, B. Stober, G.G. Fuller, A.Q. Shen, Integrated microfluidic platform for instantaneous flow and localized temperature control, RSC Adv. 5 (2015) 85620–85629. doi:10.1039/C5RA19944A.

[18] T. Pennell, T. Suchyna, J. Wang, J. Heo, J.D. Felske, F. Sachs, et al., Microfluidic chip to produce temperature jumps for electrophysiology, Anal. Chem. 80 (2008) 2447–2451. doi:10.1021/ac702169t.

[19] A.I.K. Lao, T.M.H. Lee, I.M. Hsing, N.Y. Ip, Precise temperature control of microfluidic chamber for gas and liquid phase reactions, Sensors Actuators, A Phys. 84 (2000) 11–17. doi:10.1016/S0924-4247(99)00356-8.

[20] N. Crews, C. Wittwer, B. Gale, Continuous-flow thermal gradient PCR, Biomed. Microdevices. 10 (2008) 187–195. doi:10.1007/s10544-007-9124-9.

[21] B.L. R. Zhong, X. Pan, L. Jiang, Z. Dai, J. Qin, Simply and reliably integrating micro heaters / sensors in a monolithic PCR-CE microfluidic genetic analysis system, Electrophoresis. (2009) 1297–1305. doi:10.1002/elps.200800491.

[22] R. Phatthanakun, P. Deekla, W. Pummara, C. Sriphung, C. Pantong, N. Chomnawang, Fabrication and Control of Thin-Film Aluminum Microheater and Nickel Temperature Sensor, Circuits Syst. Adv. Technol. (2011) 14–17.

[23] K. Jensen, D. Ph, K.F. Jensen, Temperature Microreactors

for Nanostructure Synthesis, J. Assoc. Lab. Autom. 14 (2009) 367–373. doi:10.1016/j.jala.2009.06.005.
[24] S.K. Luther, A. Braeuer, The Journal of Supercritical Fluids High-pressure microfluidics for the investigation into multi-phase systems using the supercritical fluid extraction of emulsions (SFEE), J. Supercrit. Fluids. 65 (2012) 78–86. doi:10.1016/j.supflu.2012.02.029.
[25] M.H. Winer, A. Ahmadi, K.C. Cheung, Lab on a Chip tracking method to microfluidic particle focusing †, (2014) 1443–1451. doi:10.1039/c3lc51352a.
[26] R.G. Geitenbeek, Catalyst Particle-embedded Luminescent Nanoparticles for Temperature Sensing, (2016). http://www.mcec-researchcenter.nl/projects/catalyst-particle-embedded-luminescent-nanoparticles-for-temperature-sensing/ (accessed June 27, 2016).

SUPPLEMENTARY INFORMATION

SI.1 Clarifications on calculations and choices made in the simulation process

SI1.1 Simulation geometry

For an estimation of the amount of power that is needed to heat up the fluids in the channel, a COMSOL simulation has been performed. Figure 1.1 shows the geometry of the device. Because of the symmetry of both heater and channel, only half of the channel is simulated. Further included in the geometry are the silicon wafer (3), the fluid (water) that is present in the channel (2) and the platinum heater element (1). This is a simplified representation of the design, whereas in the actual design the wall of the channel would contain a second phase for the droplets, a thin insulating layer of 200 nm silicon dioxide, more bulk silicon, and a glass layer on top. All the simplifications mentioned above are done to reduce the simulation time.

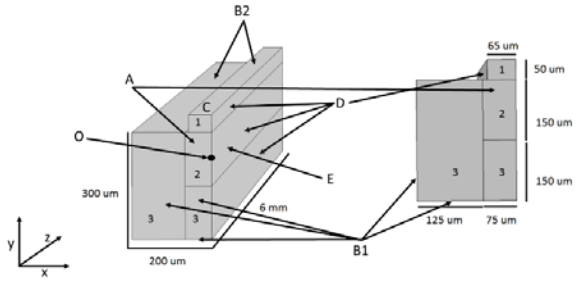

Figure 1.1: Geometry used in the COMSOL simulation showing materials, dimensions, and boundary conditions that are used. Materials being platinum (1), water (2), and silicon (3). Boundary conditions are: Inlet parabolic velocity profile for the fluidic channel (A), heat loss modelled as an outflux of 953 $\mathrm{Wm^{-2}K^{-1}}$ (B1) and 10 $\mathrm{Wm^{-2}K^{-1}}$ (B2), Heat source of 300 mW (C), Thermally insulating surfaces (D), and no viscous stress (E) on the appointed channel wall. (O) marks the origin of the channel. (S) marks the symmetry planes of the geometry.

S1.2 Heat loss estimation

The heat transfer coefficient, h in $\mathrm{Wm^{-2}K^{-1}}$, that represents the amount of silicon and glass that is exposed to air is calculated and used to give a value for the outflux oF heat per channel wall.

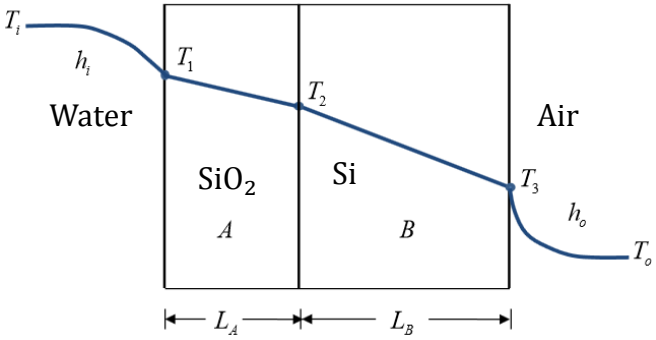

Figure 1.2: Model used for calculating the convective and conductive heat transfers, seen as a series of thermal resistances. The total heat transfer coefficient from fluid at temperature $\mathrm{T_i}$ through solids A ($\mathrm{SiO_2}$) and B (Silicon), towards the output temperature $\mathrm{T_o}$ at ambient air is estimated using the model. $\mathrm{h_i}$ and $\mathrm{h_o}$ are the heat transfer coefficients of water and air. $\mathrm{T_1}$, $\mathrm{T_2}$, and $\mathrm{T_3}$ are the temperatures at the surfaces of solids A and B, and finally $\mathrm{L_A}$ and $\mathrm{L_B}$ are the lengths of the respective solids. Image is used form [1]

Figure 1.2 shows a 2D model of the heat losses going from the fluid in the channel $\mathrm{T_i}$ on the left, through two solid layers (A and B), ending on the right side at $\mathrm{T_o}$. This model is used to calculate the steady state power Q (W). In the microheater system this would mean that the fluid on the left is water, block A is the silicon dioxide layer, B is the bulk silicon, and air on the right side. Equation (1) below from [1] describes the relation for calculating the power in this system.

$$\mathrm{Q = UA(T_i - T_0)} \qquad (1)$$

In which U is the overall heat transfer coefficient in $\mathrm{Wm^{-2}K^{-1}}$, A is the surface area in $\mathrm{m^2}$, T is the temperature in K. U can be further expressed as in equation (2) [1], where it is the summation of all individual thermal resistances of the different blocks.

$$\frac{1}{\mathrm{U}} = \frac{\mathrm{L_{water}}}{\mathrm{k_{water}}} + \frac{\mathrm{L_{SiO_2}}}{\mathrm{k_{SiO_2}}} + \frac{\mathrm{L_{Si}}}{\mathrm{k_{Si}}} + \frac{1}{\mathrm{h_{air}}} \qquad (2)$$

In which k ($\mathrm{Wm^{-1}K^{-1}}$) and L (m) are the thermal conductivity and length of each individual block, and $\mathrm{h_0}$ $\mathrm{Wm^{-2}K^{-1}}$ is the heat transfer coefficient of air, which is 10 $\mathrm{Wm^{-2}K^{-1}}$. The calculation shows that the overall heat transfer coefficient is mostly determined by the transition from silicon to air, since it has the highest thermal resistance, limiting the heat flow the most.

In the this 2D model only the heat loss through the side of the channel is calculated, so for the total surface area, also the top and bottom are taken into account. The eventual chip will be 15mmx20 mmx1mm, and because of the symmetry, only half of its surface area is used in the model to calculate the heat losses. The total surface area that is in contact with the air for said chip is $3 * 10^{-4}\ \mathrm{m}^2$. In steady state the heat flow, as well as the internal and external temperature, is constant. In order for the small scale COMSOL model to reach the same steady state level, the heat transfer coefficient times the area through which heat is lost, should be constant as well. With the calculated heat flux coefficient for the aforementioned area, the small scale heat flux coefficient can be calculated with the dimensions of the geometry of the model from Figure 1.1. Subsequently resulting in an equivalent model area of $3.15 * 10^{-6}\ \mathrm{m}^2$. For the walls in direct contact with air, as seen in Figure 1.1, a heat flux coefficient of 10 $\mathrm{Wm^{-2}K^{-1}}$ is used. The heat loss coefficient for the walls representing a larger area are then:

$$\mathrm{U_{model}} = \frac{3 * 10^{-4} * 10}{3.15 * 10^{-6}} = 953 \frac{\mathrm{W}}{\mathrm{m^2 K}}$$

The model is solved for a stationary study with the heat transfer module, laminar flow model, and Multiphysics for non-isothermal flow.

The resulting parabolic flow profile that was obtained with equation (3), and is shown in Figure 1.3. Here it can be seen that the "half" parabolic flow profile has its maximum at the symmetry line, indicated with an 'S' in Figure 1.3.

$$\mathrm{v_z} = \frac{9}{4}\frac{\mathrm{Q_f}}{\mathrm{HW}}\left(1 - 4\left(\frac{\mathrm{y_0 + \Delta y}}{\mathrm{H}}\right)^2\right)\left(1 - 4\left(\frac{\mathrm{x_0 + \Delta x}}{\mathrm{W}}\right)^2\right) \qquad (3)$$

Where $\mathrm{v_z}$ is the velocity in the z-direction in $\mathrm{ms^{-1}}$, H is the height of the channel in m, W is the width of the channel in m, $\mathrm{y_0}$ and $\mathrm{z_0}$ are at the origin of the channel, which indicated with an 'O' in Figure1.1, $\mathrm{Q_f}$ is the flow rate in $\mathrm{m^3 s^{-1}}$. The walls of the channel were given no slip condition, meaning that v = 0 at the walls. Boundary conditions are clarified in Figure 1.1. The temperature distribution through the whole geometry is shown in Figure 1.4 .Furthermore, in Figure 1.5 the temperature gradient from top to bottom of the channel can be seen. The line is also taken at the symmetry line 'S'.

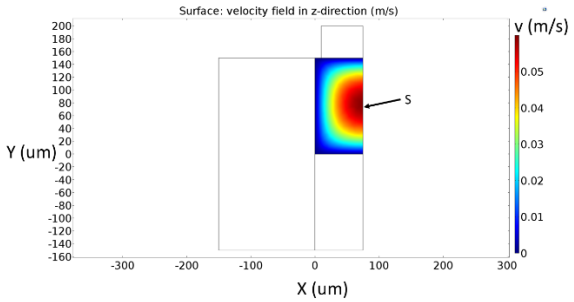

Figure 1.3: Simulation result of the flow velocity inside the channel. The velocity field at the inlet is given in equation (3)

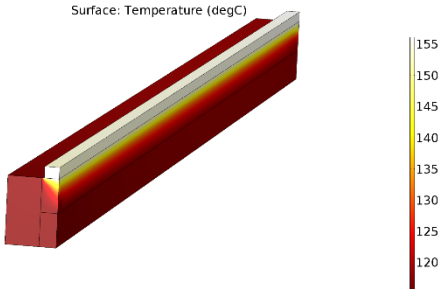

Figure 1.4: Temperature distribution through the for the complete geometry. Temperature is uniform along the symmetry line.

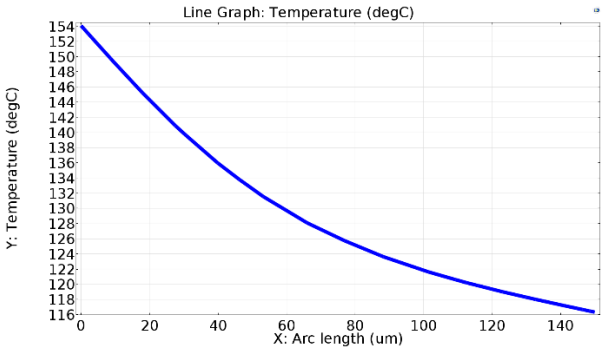

Figure 1.5: Temperature gradient inside the channel from top to bottom taken between the points (x,y), (75,150) to (75,150) seen in Figure 1.3 . All numbers are in microns.

Because the sides of the heating element are made thermally insulating and the heat loss through the top of the heater is small compared to the heat exchange between the channel and the heater, the power per unit area (the contact area between the heater and the channel) can be calculated with the simulation results. In the simulation this means that there is 6.67e5 $\mathrm{W/m^2}$. Using the contact area between the heater and the channel from the design, approximately 1.13 W is needed to heat the channel up to 155 °C, according to the simulation.

SI.2 Masks used in fabrication process

The masks used in the process flow are shown below in Figure 2.1Figure 2.2, and Figure 2.3 and were made in Clewin. The first mask (Figure 2.1) is used for creating the thin film structures, like the heaters and sensors in the glass substrate. The second mask (Figure 2.2) is used to etch channel structures in the silicon substrate, and finally the third mask (Figure 2.3) is used to create electronic and fluidic accesses in the silicon substrate. These masks are used in the process flow listed in Supplementary Information (SI.6). In the comment section of the process flow the mask number that is used for each lithography step is listed.

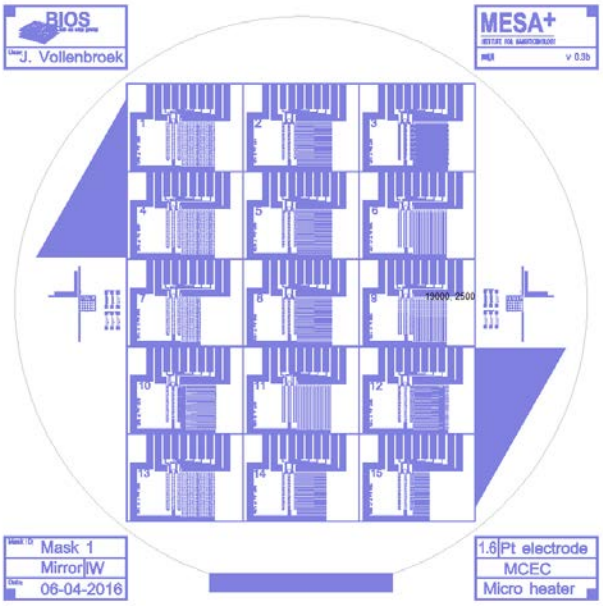

Figure 2.1: Mask 1 used for patterning of thin film structures on the glass substrate

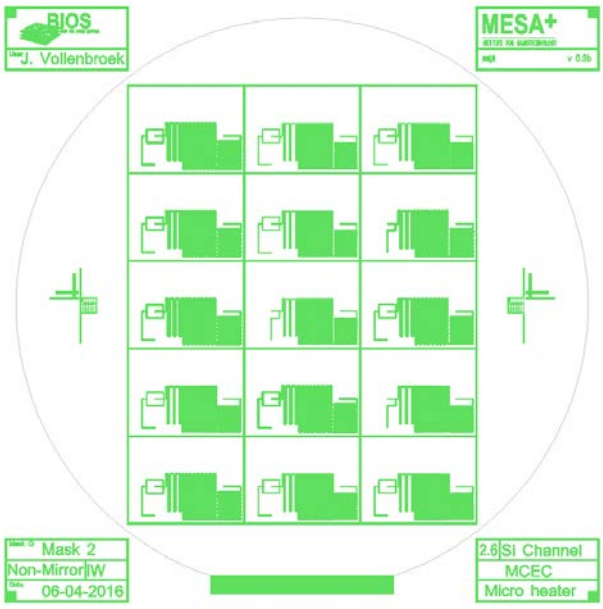

Figure 2.2: Mask 2, used for patterning of the fluidic channels in the silicon substrate

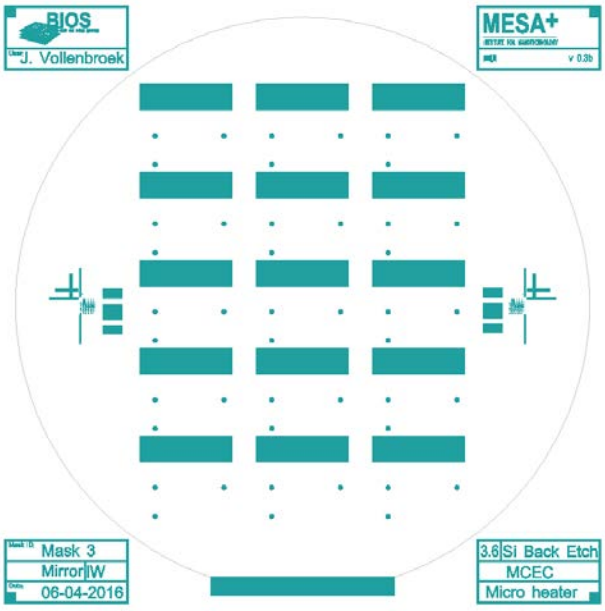

Figure 2.3: Mask 3, used for patterning of the electrical and fluidic accesses.

SI.3 Electrical circuits used for measurement and control

Schematic of the temperature sensor read-out circuit Figure 3.1 and heater control circuit Figure 3.2 will be explained. In the sensor read-out structure, the LM317TG is used as a current source. The formula for the output current is given by equation (4).

$$I_{out} = \frac{1.25}{R_1} \quad (4)$$

I_{out} is chosen to be 2 mA as to not heat up the structure by this bias current. This makes R_1 625 Ω. The current through the sensor causes a voltage drop across the resistors. This voltage is amplified using a AD620ANZ instrumentation amplifier. The formula used in calculating the gain of this amplifier is shown in equation (5).

$$Gain = \frac{49.4}{R_{Gain}} + 1 \quad (5)$$

The gain is chosen in such a way that the voltage across at the output of the amplifier would be 5V when the resistor has a temperature of 250 °C. This was done get enough gain in the desired temperature range, but to have some margin with the upper limit of the 12 bit ADC of the myRio. These considerations result in a gain of 82, making R_{gain} 610 Ω. The 12 bit ADC and the choices for the gain of the instrumentation amplifier result in a resolution of 0.15 °C for the whole sensor circuit.

For the heater actuation a PI control is used, executed by the myRio board. The circuit in Figure 3.2 shows how control is done. The gate of the NMOS is connected to the PWM output port of the myRio. Depending on the temperature setpoint, controlled in the software, the myRio controls the duty cycle of a 1 kHz square wave coming out of the PWM port. A duty cycle value of 1 means a DC voltage of 3.3 V, and a duty cycle of 0 means 0 V on the gate of the NMOS. Heaters H1 and H2 are connected to the same NMOS, because they are so close together that it is not possible to set them both at a completely different temperature, without influencing each other's read-out.

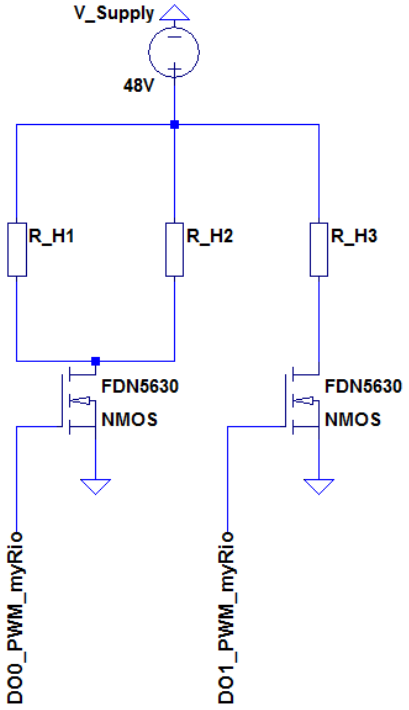

Figure 3.2: Electrical circuit used in the control of the power in the heater H1, H2, and H3.

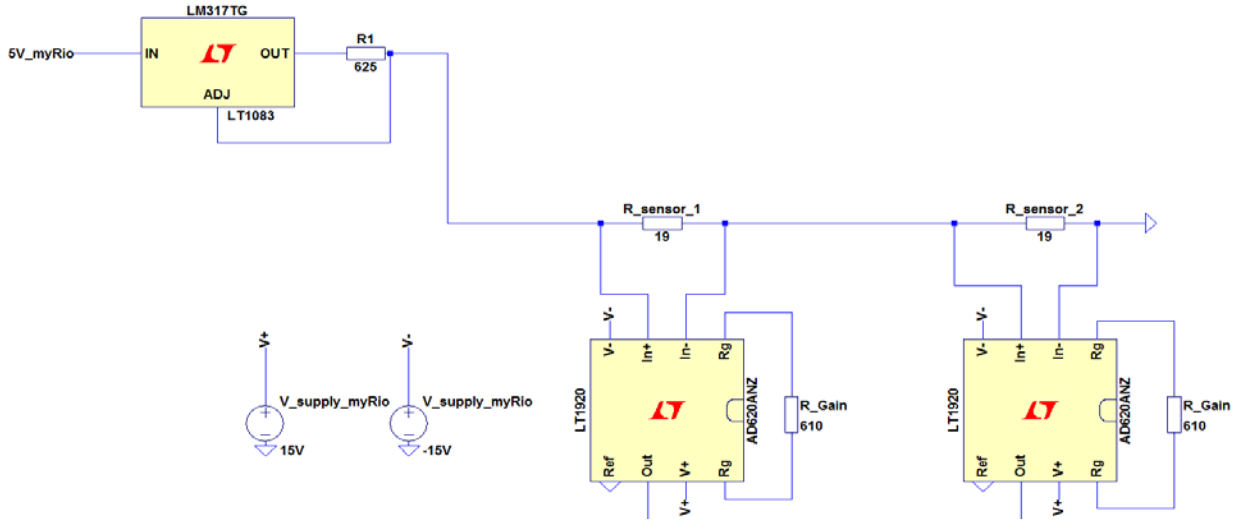

Figure 3.1: Electrical read-out circuit used in amplification and measurement of the voltage across the temperature sensor structures S1 and S2.

SI.4 Temperature sensor characterization of S2, and control measurements of heaters H1, H2 and H3

SI.4.1 Temperature sensor (S2) characterization

The temperature characteristic of S2 is given in this Supplementary information. The characterization is done in the same experiment as for S1, with the oil immersion method. Figure 4.1 shows the graph that was obtained for R2. It has a sensitivity of 0.0476 $\Omega°C^{-1}$, which is the same as for S1, and an offset of 18.294 Ω. The measure of linearity, R^2, is 0.9989.

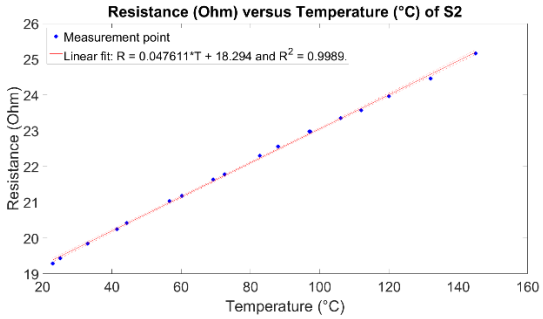

Figure 4.1: Temperature characteristic of S2

SI.4.2 Control of H1 and H2

Figure 4.2 and Figure 4.3 show the temperature readout of both sensors (S1 and S2) and the corresponding duty cycle applied to the gate of the NMOS, for a transient response from 50 °C to 75 °C.

The mean temperature value of the part starting at 18.6 seconds and ending at 39 seconds in Figure 4.2 is 76.03 °C with a standard deviation of 2.56 °C. The same interval for Figure 4.3 gives a mean of 76.51 °C and a standard deviation of 2.60 °C. The power used in heating the chip is calculated with the resistance of the heater, the duty cycle, and the voltage across the resistor. The calculation shows that 530 mW is needed to reach 50 °C.

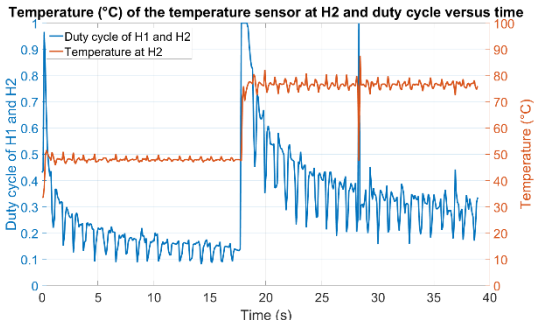

Figure 4.2: Step response of the control loop showing the temperature at H2 and the duty cycle controlling the power in H2. After 18 seconds the setpoint was changed from 50 °C to 75 °C.

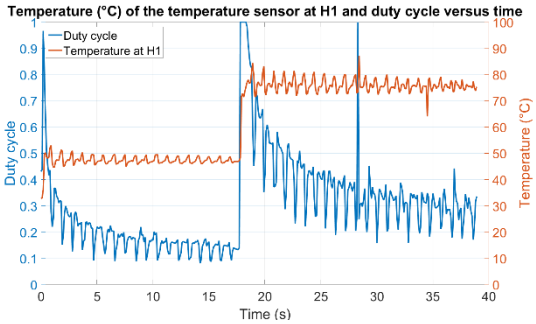

Figure 4.3: Step response of the control loop showing the temperature at H1 and the duty cycle controlling the power in H1. After 18 seconds the setpoint was changed from 50 °C to 75 °C.

SI.4.3 Control of H3

The parallel heaters (H3) can be controlled via the Labview software. They are connected to a different NMOS than H1 and H2. In the software the duty cycle can be adjusted. Figure 4.4 illustrates the influence of the parallel heaters on the control loop.

During this experiment the duty cycle of H3 is gradually increased. In the beginning the temperature is mainly maintained by H1 and H2, but when the duty cycle of H3 is increased, it is visible that the duty cycle of H1 and H2 is going down. This is starting around t1. At t2 the duty cycle for H1 and H2 is 0, but the temperature increases. The increase comes from the heat generated solely by H3. By decreasing the duty cycle of H3 again, the temperature can be made constant around the setpoint, as shown at t3. The ideal duty cycle for H3 can be manually determined by looking at the behaviour of the system.

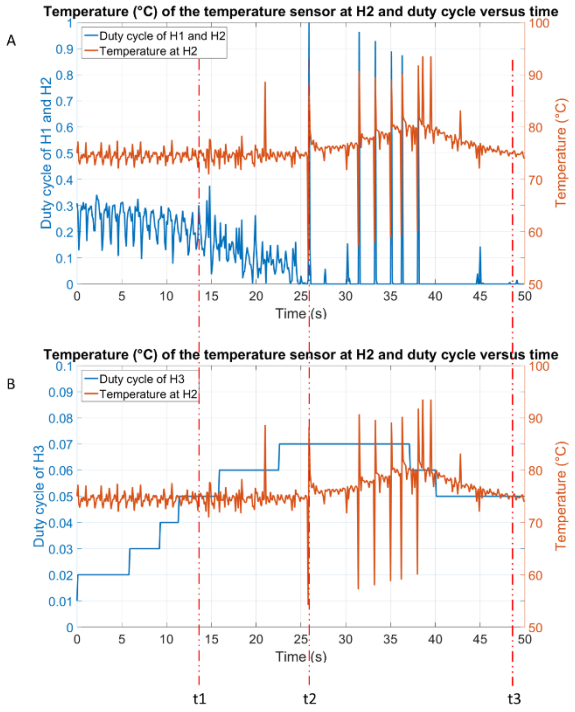

Figure 4.4: Temperature of H2 dependent on activation of A) The duty cycle controlling H1 and H2 and B) The duty cycle controlling H3. At t1 the duty cycle of H1 and H2 starts to decrease and at t2 it is 0. From t2 the temperature at H2 increases as a result of the heat produced by H3. Finally at t3 the duty cycle of H3 has been adjusted to maintain the temperature at the pre-set level of 75 °C.

SI.5 Droplet monodispersity

Images of droplets at different flow rates were taken and the volumes of the droplets are compared within and between experiments. The ratio of flow rates between the water and oil phase was kept constant during the experiments, being water:oil 3:1. Flow rates of 9 vs 3 $\mu L/min$, 45 vs 15 $\mu L/min$, and 90 vs 30 $\mu L/min$, were tested. The results are shown in Figure 5.1 . It can be seen that the volume of the droplets decreased when the flow rate goes up. The volume was calculated with the height width of the channel being 150 μm and 250 μm respectively. The length was calculated by looking at how many segments of the heater the droplet spanned. Volume of the droplets was 21 pL, 14 pL, and 11 pL. Within the measurements the monodispersity of the droplets was high, as shown in Figure 5.1.

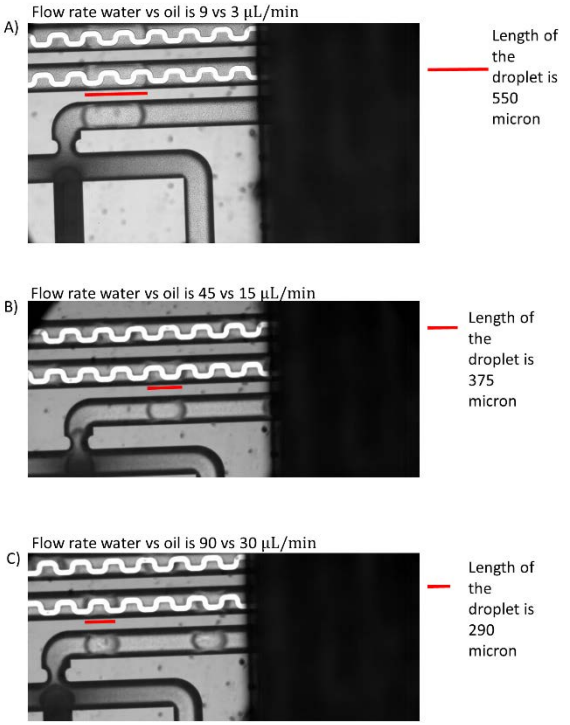

Figure 5.1: Droplets created at different flow rates for the water and oil phase. Flow rate ratio is kept equal, being water:oil 3:1

SI.6 Process flow

Name of process flow:	Droplet microreactor
Platform:	Fluidics
Creation date:	2016-06-23
Personal information	
User name:	Vollenbroek, Jeroen (BIOS)
Email address:	j.c.vollenbroek@student.utwente.nl
Company/Chair:	Masterstudenten
Function:	Other
Project:	MCEC Droplet platform
Name of supervisor:	Mathieu Odijk
Process planning	
Process start:	2016-04-04
Process end:	2016-04-18
Status	
Name of advisor:	Bruinink, Christiaan (MESA)
Last revision:	2016-06-23
Approval:	
Approval date:	
Expiration date:	

ILP: In-line Processing	MFP: Metal-free Processing	UCP: Ultra Clean Processing	Removal of Residues

Step	Level	Process/Basic flow		User comments
1		**Substrate Silicon** (#subs101)	NL-CLR-Wafer Storage Cupboard Orientation: <100> Diameter: 100mm Thickness: 525µm +/- 25µm Polished: Single side (OSP) Resistivity: 5-10Ωcm Type: p/boron	
litho1801: Lithography of Olin Oir 907-17 (positive resist - ILP)				

2	ILP	**Dehydration bake** (#litho001)	NL-CLR-WB21/22 Dehydration bake on hotplate • Temperature: 120°C • Time: 5min After the dehydration bake, perform the wafer priming with minimum delay!	
3	ILP	**Priming HMDS (liquid)** (#litho600)	NL-CLR-WB21/22 Coating: Primus Spinner • HexaMethylDiSilazane (HMDS) • Spin program: 4000 (4000rpm, 30sec)	
4	ILP	**Coating of Olin OiR 907-17** (#litho101)	NL-CLR-WB21 Coating: Primus spinner • Olin OiR 907-17 • Spin program: 4000 (4000rpm, 30sec)	2000 rpm instead of 4000 rpm
5	ILP	**Prebake of Olin OiR 907-17** (#litho003)	NL-CLR-WB21 Prebake: Hotplate • Temperature: 95°C • Time: 90s	
6	ILP	**Alignment & exposure of Olin OiR 907-17** (#litho301)	NL-CLR- EV620 Electronic Vision Group EV620 Mask Aligner • Hg-lamp: 12 mW/cm ^{2} • Exposure time: 4sec	MASK2
7	ILP	**After exposure bake of Olin OiR resists** (#litho005)	NL-CLR-WB21 After exposure bake: Hotplate • Temperature: 120°C • Time: 60s	
8	ILP	**Development of Olin OiR resists** (#litho200)	NL-CLR-WB21 Development: OPD4262 • Beaker 1: 30sec • Beaker 2: 15-30sec	
9	ILP	**Quick Dump Rinse (QDR)** (#rinse119)	NL-CLR-Wetbenches Purpose: removal of traces of chemical agents. Recipe 1 Quick dump rinsing (QDR) Recipe 2 Cascade rinsing for fragile wafers Rinse until message ´End of rinsing process´ is shown on the touchscreen of the QDR, else repeat the rinsing process.	
10	ILP	**Substrate drying** (#dry120)	NL-CLR-WB **Single substrate drying:** 1. Use the single-wafer spinner Settings: 2500 rpm, 60 sec (including 45 sec nitrogen purge) 2. Use the nitrogen gun (fragile wafers or small samples)	

11	ILP	**Postbake of Olin OiR resists** (#litho008)	NL-CLR-WB21 Postbake: Hotplate • Temperature: 120°C • Time: 10min	
12	ILP	**Inspection by optical microscope** (#metro101)	NL-CLR- Nikon Microscope • dedicated microscope for lithography inspection	

etch1650: DRIE of silicon: Bosch high rate STD (SPTS Pegasus)

13 ILP

DRIE of silicon STD high rate
(#etch212)

NL-CLR-SPTS Pegasus
Bosch High rate for micro features

Platen temp: -19°C - He pres: 20Torr

Parameters	Etch	Deposition
Gas	SF6	C4F8
Flow [sccm]	800	400
Boost Flow [sccm - sec]	350 - 1,5	-
Time [sec]	7	2
APC [%]	8	8
ICP [Watt]	3000	3000
CCP [Watt]	40 (RF)	
Boost CCP [Watt - sec]	300 - 2,5	-

Etch rate Si: 20-30 um/min

At first try 1.7 micron resist was not enough to etch 150 micron channels. Resist rate estimated at 120nm/min. Process time for channels is 16 minutes.

14 ILP

SPTS Pegasus chamber/chuck clean
(#etch219)

NL-CLR-SPTS Pegasus)
Name: TDSec clean

Parameters:
Flow: 200 sccm O2
Pressure: 5 mTorr
ICP: 2500W
CCP: 20W (RF)
15 minutes after use
After cleaning the substrate holder temp will be set tot 20°C

The 3 min version will not change the temperature

15 Rem Res

Removal of Fluorocarbon
(#residue104)

NL-CLR-TePla 360
Purpose: removal of Fluorocarbon in O_2/CF_4 Plasma after BOSCH etching, including any resists present on the substrate.

WARNING: this recipe also attacks silicon and nitride coatings for several nanometers!

			Recipe 071 **1- Removal of Resists** O_2 flow: 500sccm Pressure: 0.8mbar (35% valve) Power: 600Watt Time: 20 min **2- Removal of Fluorocarbon** O_2 flow: 475sccm CF_4 flow: 25sccm Pressure: 0.8mbar (35% valve) Power: 800Watt Time: 1min **3- Removal of residual Fluorocarbon** O_2 flow: 500sccm Pressure: 0.8mbar (35% valve) Power: 800Watt Time: 1min	
litho1802: Lithography of Olin Oir 908-35 (positive resist - ILP)				
16	ILP	**Dehydration bake** (#litho001)	NL-CLR-WB21/22 Dehydration bake on hotplate • Temperature: 120°C • Time: 5min After the dehydration bake, perform the wafer priming with minimum delay!	
17	ILP	**Priming HMDS (liquid)** (#litho600)	NL-CLR-WB21/22 Coating: Primus Spinner • HexaMethylDiSilazane (HMDS) • Spin program: 4000 (4000rpm, 30sec)	
18	ILP	**Coating of Olin OiR 908-35** (#litho102)	NL-CLR- WB21 Coating: Primus coater • Olin OiR 908-35 • Spin program: 4000 (4000rpm, 30sec)	Use 2000 rmp instead of 4000 rpm
19	ILP	**Prebake of Olin OiR 908-35** (#litho004)	NL-CLR-WB21 Prebake: Hotplate • Temperature: 95°C • Time: 120s	
20	ILP	**Alignment & exposure of Olin OiR 908-35** (#litho302)	NL-CLR- EV620 • Electronic Vision Group EV620 Mask Aligner • Hg lamp: 12 mW/cm ^{2} • Exposure time: 9sec	MASK 3

21	ILP	**After exposure bake of Olin OiR resists** (#litho005)	NL-CLR-WB21 After exposure bake: Hotplate • Temperature: 120°C • Time: 60s	
22	ILP	**Development of Olin OiR resists** (#litho200)	NL-CLR-WB21 Development: OPD4262 • Beaker 1: 30sec • Beaker 2: 15-30sec	
23	ILP	**Quick Dump Rinse (QDR)** (#rinse119)	NL-CLR-Wetbenches Purpose: removal of traces of chemical agents. Recipe 1 Quick dump rinsing (QDR) Recipe 2 Cascade rinsing for fragile wafers Rinse until message ´End of rinsing process´ is shown on the touchscreen of the QDR, else repeat the rinsing process.	
24	ILP	**Substrate drying** (#dry120)	NL-CLR-WB **Single substrate drying:** 1. Use the single-wafer spinner Settings: 2500 rpm, 60 sec (including 45 sec nitrogen purge) 2. Use the nitrogen gun (fragile wafers or small samples)	
25	ILP	**Postbake of Olin OiR resists** (#litho008)	NL-CLR-WB21 Postbake: Hotplate • Temperature: 120°C • Time: 10min	
26	ILP	**Inspection by optical microscope** (#metro101)	NL-CLR- Nikon Microscope • dedicated microscope for lithography inspection	

etch1506: DRIE of Silicon: A-pulsed-C4F8 STD (AdixenSE)

27	ILP	**DRIE of Si A pulsed C4F8 at -40°C** (#etch175)	NL-CLR-Adixen SE Application: trenches, wafer through using thick photoresist (908-35) Use: C4F8 flow and CCP for tuning process. SH temp: -40°C - Pos: 110mm - He pres: 10mbar	Use foil on top of wafer to prevent He leak.

Parameters	**Etch**	**Deposition**
Gas	SF_6	C_4F_8
Flow (sccm)	**500**	**175**
Time (sec)	4	0.5
Priority	2	1
APC %	15	15
ICP (Watt)	2500	2500
CCP (Watt)	20	20
Pulsed (msec)	20on/80off	20on/80off

CCP [w]	On/off[msec]	C4F8 [sscm]	Er resist nm/min	silicon {um/min]
20	20/180	20	33-50	10
20	35/165	25	80	10

28 Rem Res

Removal of Fluorocarbon
(#residue103)

NL-CLR-TePla 360
Purpose: removal of Fluorocarbon in O_2/CF_4 Plasma after BOSCH etching, including any resists present on the substrate.

WARNING: this recipe also attacks silicon and nitride coatings for several nanometers!

1- Preheating
Ar flow: 600sccm
Pressure: 0.6mbar
Power: 1000Watt
Time: 10min

2- Removal of Resists
O_2 flow: 250sccm
Pressure: 0.5mbar (35% valve)
Power: 800Watt
Time: depending on recipe*

3- Removal of Fluorocarbon
O_2 flow: 237sccm
CF_4 flow: 13sccm
Pressure: 0.5mbar (35% valve)
Power: 800Watt
Time: 1min

4- Removal of residual Fluorocarbon
O_2 flow: 250sccm
Pressure: 0.8mbar (30% valve)
Power: 800Watt
Time: 1min

* Select one of the following recipes to remove the fluorocarbon and strip resists, depending on the thickness of the resist, treatment of the resist and the number of wafers.

Recipe 035: time = 10 min
Recipe 037: time = 20 min

film1685: Dry oxidation of silicon at 1100 C (H1)

29 MFP

Cleaning in 99% HNO_3
(#clean001)

NL-CLR-WB14
Purpose: removal of organic traces.

• Beaker 1: 99% HNO_3
• Time = 5 min

30	MFP	**Cleaning in 99% HNO_3** (#clean002)	NL-CLR-WB14 Purpose: removal of organic traces. • Beaker 2: 99% HNO_3 • Time = 5 min	
31	MFP	**Quick Dump Rinse (QDR)** (#rinse120)	NL-CLR-Wetbenches Purpose: removal of traces of chemical agents. Recipe 1 Quick dump rinsing (QDR) Recipe 2 Cascade rinsing for fragile wafers Rinse until message ´End of rinsing process´ is shown on the touchscreen of the QDR, else repeat the rinsing process.	
32	MFP	**Cleaning in 69% HNO_3 at 95 °C** (#clean003)	NL-CR-WB14 Purpose: removal of metallic traces. • Beaker 3A or 3B: 69% HNO_3 • Temperature= 95 °C • Time = 10 min	
33	MFP	**Quick Dump Rinse (QDR)** (#rinse120)	NL-CLR-Wetbenches Purpose: removal of traces of chemical agents. Recipe 1 Quick dump rinsing (QDR) Recipe 2 Cascade rinsing for fragile wafers Rinse until message ´End of rinsing process´ is shown on the touchscreen of the QDR, else repeat the rinsing process.	
34	MFP	**Substrate drying (WB14)** (#dry159)	NL-CLR-WB14 Optional drying step. After the QDR, you can transfer your substrates directly to a Teflon carrier and strip the native SiO2 in 1% HF (WB15). **Single substrate drying:** 1. Use the single-wafer spinner Settings: 2500 rpm, 60 sec (including 45 sec nitrogen purge) 2. Use the nitrogen gun (fragile wafers or small samples) **Batch drying of substrates:** The Semitool uses the following standard procedure: • Rinse: 30 sec (600 rpm) • Q-rinse: 10.0 MΩ (600 rpm) • Purge: 10 sec (600 rpm) • Drying: 280 sec (1600 rpm) Note: it is obligatory to apply a single rinsing step in the QDR before using the Semitool!	Optional: transfer your wafers directly from the QDR into the 1% HF solution to the native SiO2.
35	MFP	**Etching in 1% HF** (#etch127)	NL-CLR-WB15 Purpose: remove native SiO2 from silicon.	Obligatory for the silicon

			Beaker: 1% HF Temperature: room temperature Time = 1 min This step is obligatory for the MESA+ monitor wafer (if applicable, see Equipment database).	monitor wafer of the furnace (if applicable).
36	MFP	**Quick Dump Rinse (QDR)** (#rinse120)	NL-CLR-Wetbenches Purpose: removal of traces of chemical agents. Recipe 1 Quick dump rinsing (QDR) Recipe 2 Cascade rinsing for fragile wafers Rinse until message ´End of rinsing process´ is shown on the touchscreen of the QDR, else repeat the rinsing process.	
37	MFP	**Substrate drying (WB15)** (#dry160)	NL-CLR-WB15 **Single substrate drying:** 1. Use the single-wafer spinner Settings: 2500 rpm, 60 sec (including 45 sec nitrogen purge) 2. Use the nitrogen gun (fragile wafers or small samples) **Batch drying of substrates:** The Semitool uses the following standard procedure: • Rinse: 30 sec (600 rpm) • Q-rinse: 10.0 MΩ (600 rpm) • Purge: 10 sec (600 rpm) • Drying: 280 sec (1600 rpm) <u>Note</u>: it is obligatory to apply a single rinsing step in the QDR before using the Semitool!	
38	MFP	**Dry oxidation of silicon @ 1100°C** (#film191)	NL-CLR-Furnace H1 • Standby temperature: 700°C • **Program: xxxx** • Temp.: 1100°C • Gas: O_2 • Flow: ?l/min	200 nm thickness. Oxidation time = 2 hour 20 min.
239		**Substrate MEMpax** (#subs117)	NL-CLR-Cupboard Diameter: 100mm Thickness: 500µm	
litho1801: Lithography of Olin Oir 907-17 (positive resist - ILP)				
40	ILP	**Dehydration bake** (#litho001)	NL-CLR-WB21/22 Dehydration bake on hotplate • Temperature: 120°C • Time: 5min After the dehydration bake, perform the wafer priming with minimum delay!	

41	ILP	**Priming HMDS (liquid)** (#litho600)	NL-CLR-WB21/22 Coating: Primus Spinner • HexaMethylDiSilazane (HMDS) • Spin program: 4000 (4000rpm, 30sec)	
42	ILP	**Coating of Olin OiR 907-17** (#litho101)	NL-CLR-WB21 Coating: Primus spinner • Olin OiR 907-17 • Spin program: 4000 (4000rpm, 30sec)	
43	ILP	**Prebake of Olin OiR 907-17** (#litho003)	NL-CLR-WB21 Prebake: Hotplate • Temperature: 95°C • Time: 90s	
44	ILP	**Alignment & exposure of Olin OiR 907-17** (#litho301)	NL-CLR- EV620 Electronic Vision Group EV620 Mask Aligner • Hg-lamp: 12 mW/cm ^{2} • Exposure time: 4sec	MASK 1
45	ILP	**After exposure bake of Olin OiR resists** (#litho005)	NL-CLR-WB21 After exposure bake: Hotplate • Temperature: 120°C • Time: 60s	
46	ILP	**Development of Olin OiR resists** (#litho200)	NL-CLR-WB21 Development: OPD4262 • Beaker 1: 30sec • Beaker 2: 15-30sec	
47	ILP	**Quick Dump Rinse (QDR)** (#rinse119)	NL-CLR-Wetbenches Purpose: removal of traces of chemical agents. Recipe 1 Quick dump rinsing (QDR) Recipe 2 Cascade rinsing for fragile wafers Rinse until message ´End of rinsing process´ is shown on the touchscreen of the QDR, else repeat the rinsing process.	
48	ILP	**Substrate drying** (#dry120)	NL-CLR-WB **Single substrate drying:** 1. Use the single-wafer spinner Settings: 2500 rpm, 60 sec (including 45 sec nitrogen purge) 2. Use the nitrogen gun (fragile wafers or small samples)	
49	ILP	**Postbake of Olin OiR resists** (#litho008)	NL-CLR-WB21 Postbake: Hotplate • Temperature: 120°C • Time: 10min	
50	ILP	**Inspection by optical microscope** (#metro101)	NL-CLR- Nikon Microscope • dedicated microscope for lithography inspection	

etch1208: BHF etch (WB10-private use)

51	ILP	**Etching SiO2 BHF (1:7)** (#etch125)	NL-CLR-WB9 or 10 Use private beaker with BHF (1:7) Temp.: room temperature Etchrates: • thermal SiO2: 60-80nm/min • PECVD Si02: 125/nm/min • TEOS SiO2: 180/nm/min • TEOS **H3 (new):** 242 nm/min • Pyrex #7740: 20nm/min • Borofloat BF33: 20-25 nm/min • Si3N4-H2: 0.64 nm/min	Etch depth 200 nm. 8 min 40 sec
52	ILP	**Quick Dump Rinse (QDR)** (#rinse119)	NL-CLR-Wetbenches Purpose: removal of traces of chemical agents. Recipe 1 Quick dump rinsing (QDR) Recipe 2 Cascade rinsing for fragile wafers Rinse until message ´End of rinsing process´ is shown on the touchscreen of the QDR, else repeat the rinsing process.	
53	ILP	**Substrate drying** (#dry120)	NL-CLR-WB **Single substrate drying:** 1. Use the single-wafer spinner Settings: 2500 rpm, 60 sec (including 45 sec nitrogen purge) 2. Use the nitrogen gun (fragile wafers or small samples)	
		film1532: Sputtering of Tantalum (TCOathy)		
54	ILP	**Sputtering of Ta** (#film622)	**NL-CLR-T´COathy** Ta Target • Use Ar flow to adjust process pressure. • Base pressure: < 1.0 e-6mbar • Sputter pressure: 6.6 e-3mbar • power: 200W • Deposition rate = 9.4 nm/min	Thickness = 10 nm. Time = 1 min
		film1534: Sputtering of Platinum (TCOathy)		
55	ILP	**Sputtering of Pt** (#film624)	**NL-CLR-T´COathy** Pt Target • Use Ar flow to adjust process pressure. • Base pressure: < 1.0 e-6mbar • Sputter pressure: 6.6 e-3mbar • power: 200W • Deposition rate = 24.0 nm/min	Thickness = 190 nm. Time = 7 min 55 sec
		litho1500: Lift-Off with positive resist (WB11)		
56	ILP	**Lift-Off** **(#**litho500)	NL-CLR-WB11 Purpose: removal of resist and excess metal from the surface of the substrate by ultrasonication in Acetone. Use the ultrasonic bath in WB11. • Beaker 1: Acetone • Time = 10 min	

			Single wafer processing: Spray the wafer with Acetone for 30 sec and immediately spray with isopropanol (IPA) for 30 sec. **Batch wafer processing:** • Beaker 2: Acetone • Time = 10 min • Beaker 3: Isopropanol • Time = 10 min
57	ILP	**Substrate drying** (#dry120)	NL-CLR-WB **Single substrate drying:** 1. Use the single-wafer spinner Settings: 2500 rpm, 60 sec (including 45 sec nitrogen purge) 2. Use the nitrogen gun (fragile wafers or small samples)
		film1400: PECVD of SiO2 - standard (Oxford80)	
58	ILP	**Cleaning in 99% HNO_3** (#clean005)	NL-CLR-WB16 Purpose: removal of organic traces. • Beaker 1: 99% HNO_3 • Time = 5 min
59	ILP	**Cleaning in 99% HNO_3** (#clean006)	NL-CLR-WB16 Purpose: removal of organic traces. • Beaker 2: 99% HNO_3 • Time = 5 min
60	ILP	**Quick Dump Rinse (QDR)** (#rinse119)	NL-CLR-Wetbenches Purpose: removal of traces of chemical agents. Recipe 1 Quick dump rinsing (QDR) Recipe 2 Cascade rinsing for fragile wafers Rinse until message ´End of rinsing process´ is shown on the touchscreen of the QDR, else repeat the rinsing process.
61	ILP	**Substrate drying** (#dry120)	NL-CLR-WB **Single substrate drying:** 1. Use the single-wafer spinner Settings: 2500 rpm, 60 sec (including 45 sec nitrogen purge) 2. Use the nitrogen gun (fragile wafers or small samples)
62	ILP	**Chamber clean Oxford 80 PECVD** (#film194)	NL-CLR-Oxford 80 PECVD • Chamber clean

63	ILP	**PECVD of SiO_2 Standard** (#film132)	NL-CLR-OXFORD Plasmalab 80 $^+$ Apply purge sequence before and after use Purge sequence: 1 min N_2, pump down, apply three times Parameters: • Electrode temp. = 300°C • 2% SiH_4/N_2 flow = 200sccm • N_2O flow = 710sccm • pressure = 650mTorr • APC = 33 • power LF = 60W • Deposition rate= 35-40 nm/min	Thickness = 1000 min. Time = 30 min.
64	ILP	**Chamber clean Oxford 80 PECVD** (#film194)	NL-CLR-Oxford 80 PECVD • Chamber clean	
65	ILP	**Ellipsometer measurement** (#metro107)	NL-CLR-Woolam M-2000 ellipsometer	
66	ILP	**Inspection of LPCVD/PECVD layers** (#metro113)	NL-CLR-cold light source Particle and haze inspection of LPCVD/PECVD layers using a cold light source. Procedure: use streaking light for inspection. Contact: Ite-Jan/Chris for results.	
		litho1801: Lithography of Olin Oir 907-17 (positive resist - ILP)		
67	ILP	**Dehydration bake** (#litho001)	NL-CLR-WB21/22 Dehydration bake on hotplate • Temperature: 120°C • Time: 5min After the dehydration bake, perform the wafer priming with minimum delay!	
68	ILP	**Priming HMDS (liquid)** (#litho600)	NL-CLR-WB21/22 Coating: Primus Spinner • HexaMethylDiSilazane (HMDS) • Spin program: 4000 (4000rpm, 30sec)	
69	ILP	**Coating of Olin OiR 907-17** (#litho101)	NL-CLR-WB21 Coating: Primus spinner • Olin OiR 907-17 • Spin program: 4000 (4000rpm, 30sec)	
70	ILP	**Prebake of Olin OiR 907-17** (#litho003)	NL-CLR-WB21 Prebake: Hotplate • Temperature: 95°C • Time: 90s	
71	ILP	**Alignment & exposure of Olin OiR**	NL-CLR- EV620 Electronic Vision Group EV620 Mask Aligner	MASK 3

		907-17 (#litho301)	• Hg-lamp: 12 mW/cm ^{2} • Exposure time: 4sec	
72	ILP	**After exposure bake of Olin OiR resists** (#litho005)	NL-CLR-WB21 After exposure bake: Hotplate • Temperature: 120°C • Time: 60s	
73	ILP	**Development of Olin OiR resists** (#litho200)	NL-CLR-WB21 Development: OPD4262 • Beaker 1: 30sec • Beaker 2: 15-30sec	
74	ILP	**Quick Dump Rinse (QDR)** (#rinse119)	NL-CLR-Wetbenches Purpose: removal of traces of chemical agents. Recipe 1 Quick dump rinsing (QDR) Recipe 2 Cascade rinsing for fragile wafers Rinse until message ´End of rinsing process´ is shown on the touchscreen of the QDR, else repeat the rinsing process.	
75	ILP	**Substrate drying** (#dry120)	NL-CLR-WB **Single substrate drying:** 1. Use the single-wafer spinner Settings: 2500 rpm, 60 sec (including 45 sec nitrogen purge) 2. Use the nitrogen gun (fragile wafers or small samples)	
76	ILP	**Postbake of Olin OiR resists** (#litho008)	NL-CLR-WB21 Postbake: Hotplate • Temperature: 120°C • Time: 10min	
77	ILP	**Inspection by optical microscope** (#metro101)	NL-CLR- Nikon Microscope • dedicated microscope for lithography inspection	

etch1511: Etching of SiO2 or SiN: C-Ar/CHF3 (AdixenSE)

78 ILP

DRIE of SiN and SiO2 C-Multilayer
(#etch174)

NL-CLR-Adixen SE
Application: directional etch of SiRN or SiO2 layer

SH temp: 20 / -100°C - Pos: 200mm - He pres: 10mbar

Etch time 4 min and 30 sec.

Parameters	Value
Argon (sccm)	100
CHF3 (sccm)	100
APC %	100
ICP (Watt)	1200
CCP (Watt) LF	150 (Vdc=680V)

			Etch rates: SiO2: 250nm/min - SiRN: 300nm/min - Si:70-80 nm/min Resist: 160nm/min - SU8: 150nm/min
79	ILP	**Stripping of Positive Resists** (#strip130)	NL-CLR-TePla360 Purpose: Stripping of Positive Resists on specific metals in O_2/H_2 Plasma. **Recipe 041** O_2 flow: 250sccm H_2 flow: 250sccm Pressure: 0.7mbar Power: 800Watt Time: 10min
		bond1107: Wafer bonding silicon-glass with Ta/Pt structures (E2)	
80	ILP	**Cleaning in 99% HNO_3** (#clean005)	NL-CLR-WB16 Purpose: removal of organic traces. • Beaker 1: 99% HNO_3 • Time = 5 min
81	ILP	**Cleaning in 99% HNO_3** (#clean006)	NL-CLR-WB16 Purpose: removal of organic traces. • Beaker 2: 99% HNO_3 • Time = 5 min
82	ILP	**Quick Dump Rinse (QDR)** (#rinse119)	NL-CLR-Wetbenches Purpose: removal of traces of chemical agents. Recipe 1 Quick dump rinsing (QDR) Recipe 2 Cascade rinsing for fragile wafers Rinse until message ´End of rinsing process´ is shown on the touchscreen of the QDR, else repeat the rinsing process.
83	ILP	**Substrate drying** (#dry120)	NL-CLR-WB **Single substrate drying:** 1. Use the single-wafer spinner Settings: 2500 rpm, 60 sec (including 45 sec nitrogen purge) 2. Use the nitrogen gun (fragile wafers or small samples)
84	ILP	**Wafer bonding** (#bond133)	NL-CLR-Furnace E2 Application: silicon-glass bonding with Ta/Pt electrodes • Standby temperature: 400 °C • Program: • Temperature range: 600-650 °C

			• Gas: N_2 • Flow: xx l/min • Ramp: xxx°C/min • Cooldown: xxx°C/min
		back1100: Dicing of a silicon wafer	
85	ILP	**Dicing foil Nitto SWT 10** (#back103)	NL-CLR dicingroom Nitto SWT 10 dicing foil
86	ILP	**UV dicing foil (Adwill D-210)** (#back104)	Nl-CLR- Dicing foil Information: Thickness: 125um Material: 100um PET + 25um Acrylic (adhesive) Adhesion before UV: 2000 mN/25mm Adhesion after UV : 15 mN/25mm UV irradiation : Luminance > 120mW/cm^2 and Quality > 70mJ/cm^2 (wave length: 365nm)
87	ILP	**Dicing of a Silicon wafer** (#back101)	**Nl-CLR-Disco DAD dicer** Applications: Silicon wafers, bonded silicon-silicon wafers (max 1.1mm) See #back103 for laminate of Nitto STW T10 dicing foil (80 µm) See #back104 for laminate of UV dicing foil (125µm) **Parameters dicing**: Wafer work size: 110 mm for a standard 100 mm silicon wafer Max. Feed speed: 10 mm/sec X, Y values: correspond respectively to Ch1 and Ch2 and those values are determined by mask layout Saw type NBC-Z 2050 Select in blade menu: **NBC-Z-2050** **Blade info:** Exposure: 1.3 mm (maximum dicing depth for a new blade) Width: 50 um Spindle revolutions: 30. 000 rpm **Depth settings:** Maximum cut depth: 1.1 mm Foil thickness: See foil info Min. blade heigth: 50 µm

REFERENCES SUPPLEMENTARY INFORMATION

[1] R.S. Subramanian, Introduction to Heat Transfer, (n.d.) 1–17.